from the retina to the amygdala via the superior colliculus and pulvinar [2,3,6,7], there is now some debate over the details following a recent proposal that the subcortical signal pathway has a complex structure comprising several branches [8].

Representative findings in support of the subliminal processing of emotions indicate that when presented with emotional facial expressions, patients with visual cortex damage discriminated emotional valence of facial expressions in the absence of conscious visual experience [9], showed different physiological responses for each emotion [10], and had an activated subcortical pathway on functional brain imaging [11]. Such phenomena were once thought to be special examples of an otherwise hidden mechanism in healthy individuals that is only exposed by a loss of conscious visual cognition. However, this subliminal process might be utilized in healthy individuals with temporally or functionally impaired visual cognition.

One of the factors in daily life that can affect visual cognition is sleep debt. Simulation studies of sleep debt (i.e., overnight total sleep deprivation) consistently show that, in addition to a marked decline in viewing-task performance, reduced activity in the parietal and occipital lobes involved in visual cognition and attention is proportional to individual vulnerability to sleep deprivation [12]. Similar results were obtained from cognitive tasks on working memory [13], vigilance [14], language learning [15], and logical thinking [16], indicating that a decline in task performance is caused by a functional decline in visual cognition and attention due to sleep debt.

Swann et al. reported shortened response times to subliminal priming after 2 days of short sleep, and stated that a decline in high-order supraliminal function due to sleepiness activated a compensatory subliminal function [17]. Furthermore, the subliminal process might work as a system that compensates for the decline seen in the level of consciousness with strong sleepiness, a situation that poses considerable danger to survival. For example, as a prey animal, a certain rabbit species sleeps with their eyes open in the wild, during which time their electroencephalograms show brain activation due to visual stimuli [18]. This is advantageous because it enables the animals to respond quickly to an attack by natural enemies, by waking up and engaging in avoidance behavior. Subliminal hazard perception might also be preserved in humans by activation via the pathway for subliminal information during episodes of strong sleepiness.

In this study, sleep debt was simulated to determine whether an increase in sleepiness induces a decline in conscious visual cognition and attention as well as activation of subliminal emotion processing.

Methods

Ethics

This study was approved by the Ethics Committee of the National Center of Neurology and Psychiatry, Japan, and was conducted in accordance with the Declaration of Helsinki.

Participants

Participants were 14 healthy, right-handed adult men (mean ± standard deviation age, 24.1 ± 3.32 years) who provided written informed consent prior to participating in the study. The participants' sleep schedule was monitored using a sleep log and actigraph (Ambulatory Monitoring Inc., Ardsley, NY) during a 2-week period prior to the study (observational period) and during the subsequent experimental period. Sleep-onset time, wake time, and the amount of time awake in bed were calculated from actigraph data according to Cole's algorithm with optimal parameters [19], and were compared with the sleep log to confirm the absence of irregular life patterns, such as shiftwork and staying up all night. Overnight polysomnography was conducted to screen for sleep disorders during the observational period.

Exclusion criteria were as follows: mean bedtime or wakeup time during the observational period outside of the hours 23:00–02:00 and 07:00–10:00, respectively; some form of sleep disorder; serious physical complication; psychiatric disorder; ocular disease, including achromatopsia; taking medication or substances that might affect the experimental data (e.g. steroids and drugs that induce drowsiness such as hypnotics and antihistamines); having an implanted metal object such as a pacemaker; performing shiftwork; or having traveled within 3 months before the study to a country with more than a 6-hour time difference. This study also excluded individuals who consumed more than 200 mg of caffeine per day and heavy smokers who were unable to quit smoking for 5 days.

Sleep restriction protocol

All participants attended a briefing session for the study, underwent sleep electroencephalography screening during the 2-week observational period, and participated in two 5-day experimental sessions. The number of hours in bed (lights out, permission to sleep) was 8 h/day in the sleep control (SC) session and 4 h/day in the sleep debt (SD) session. Both sessions were conducted as a crossover study with a 2-week interval between the sessions. To maintain a regular lifestyle during the interval, participants were restricted from staying up all night or performing shiftwork.

In the SC session, based on the sleep log and actigram from the observational period, mean bedtime (23:00–02:00) was used as the start time for 8 h of sleep (wakeup time 07:00–10:00). In the SD session, bedtime started 4 h later

(03:00–06:00) than that in the SC session and total hours in bed were 4 h (wakeup time 07:00–10:00).

In both sessions, participants stayed home for the first 3 days and then stayed in a laboratory at the National Center of Neurology and Psychiatry for the next 2 days. To maintain a strict wakeup time at home, we sent an email alert every 4 h starting at the scheduled wakeup time until bedtime, and asked participants to answer the email immediately. In the laboratory, participants were under video camera surveillance, always assisted by a research attendant, and verbally awakened when in a drowsy state, such as when taking a nap or dozing off. During the wake period, participants were allowed to move freely around the laboratory, read and write, enjoy music and videos, play videogames, and engage in conversation with a researcher. Mineral water was always available, but caffeine and alcohol intake and heavy exercise were restricted. Ambient temperature and relative humidity in the laboratory were maintained at 25 ± 0.5°C and 50 ± 5%, respectively.

MRI and emotional face-viewing task

Magnetic resonance imaging (MRI) was performed on day 5 of each session. Participants were served the same breakfast (approximately 350-kcal sandwich) within 2 h of the wakeup time, completed a questionnaire about subjective sleepiness and mood in a room adjacent to the MRI room 2–2.5 h after the wakeup time, and underwent MRI 3–5 h after the wakeup time.

During MRI, participants viewed emotional facial expressions presented under two different conditions: (1) the conscious condition, which provided sufficient viewing time to allow supraliminal visual perception of an emotional expression; and (2) the nonconscious condition, which provided a brief viewing time to allow for subliminal perception of an emotional expression followed by a neutral expression to mask the emotional facial image (Figure 1).

From the portraits of 16 individuals (8 men, 8 women) in two standardized image sets [20,21], a total of 48 images of fearful, happy, and neutral facial expressions (16 individuals × 3 facial images per person) were selected and these images were presented after making the hair and background consistent.

(1) Under the conscious condition, a fixation image was presented for 1000 ms followed by one of the three types of facial expressions for 200 ms and then a blank image for 1000 ms. (2) Under the nonconscious condition, after presenting a fixation image for 1000 ms, one of the three types of facial expressions was presented for 26 ms, followed immediately by a neutral facial image of another person of the same sex for 173 ms (backward masking), and then by a blank image for 1000 ms (Figure 1).

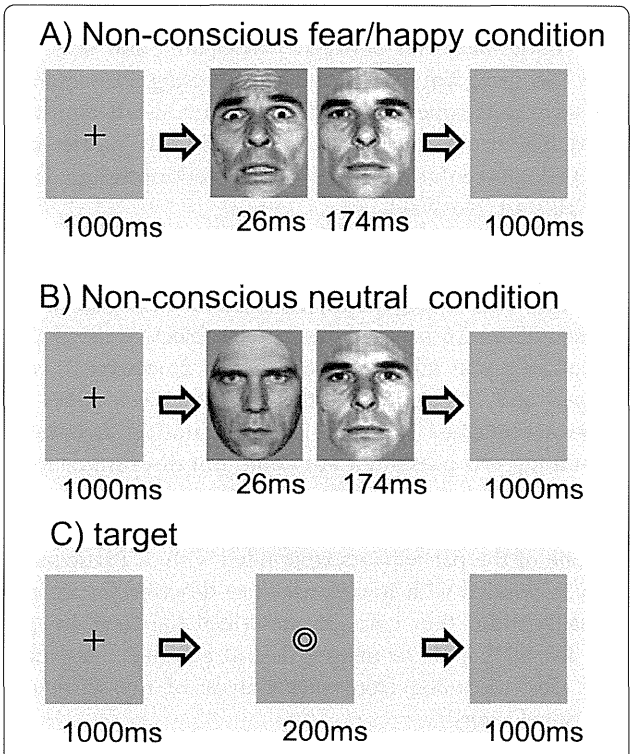

Figure 1 Schematic illustration of emotional face-viewing tasks using backward masking. A) In the nonconscious + fear task, a 26-ms presentation of a fearful face was followed by a 174-ms presentation of a neutral face of the same individual to mask the fearful face. **B)** In the nonconscious + neutral task, a 26-ms presentation of a neutral face was masked by a 174-ms presentation of a neutral face of another individual. **C)** Instead of a facial image, a specific symbol was randomly presented to maintain alertness, to which participants were asked to respond by pushing a button.

In both the conscious and nonconscious presentations, one trial consisted of presentations of a fixation image, a facial image, and a blank image. In both the conscious and nonconscious presentations, one trial consisted of presentations of a fixation image, a facial image, and a blank image. Each block consists of 9 trials of which 8 trials present either fearful, happy, or neutral facial images, and one trial shows a double circle symbol stimulus (target) used to keep participants alert and focused on the images, to which they responded by pressing a button. At the end of each block, a fixation image was shown on the screen for 15 s (baseline). A total of 12 image presentation blocks were conducted under conscious and nonconscious conditions (6 blocks each) in one session, and two sessions were performed with a 2-min break between the sessions. Each of six kinds of task block (conscious-fear, conscious-happy, conscious-neutral, nonconscious-fear, nonconscious-happy or nonconscious-neutral) was included 2 times in each

session (4 times in total). The order of block presentation was counterbalanced between participants and sessions. The task program script was coded using Presentation software (Neurobehavioral Systems Inc., www.neurobs.com). The projector's refresh rate was set to 75 Hz during task presentation (F22SX+, Projectiondesign Inc., Fredrikstad, Norway).

After completing each session, participants reported subjective sleepiness experienced during the face-viewing task and their awareness of the backward-masked image (presented for 26 ms) as follows: for subjective sleepiness, 0, not sleepy at all; 1, slightly sleepy; 2, sleepy; 3, very sleepy; and 4, slept a little; and for awareness of backward-masked images: 1, did not notice; 2, noticed something was presented but could not discriminate the faces; 3, could discriminate the faces; and 4, could see everything.

None of the participants responded with 4. Participants who responded with 3 were asked to describe the images verbally, and if they correctly described the facial images (i.e., fearful, happy, or neutral face of another individual), they were excluded from the analysis of the particular emotional category.

Three participants noticed a fearful expression image at least once, 7 participants noticed a happy expression, and one participant noticed a neutral expression (this participant also noticed a fearful face). Due to the small sample size, data for happy facial images were excluded from subsequent analyses. Eleven participants (mean ± standard deviation age, 24.5 ± 3.67 years) were unaware of the fearful or neutral facial images, and therefore only their data were analyzed.

MRI acquisition

A Siemens Magnetom Verio 3 T MRI system was used to obtain MR images. To obtain reference images for analysis, structural images (T1-weighted magnetization-prepared rapid gradient-echo [MPRAGE] images) were taken with the following sequence parameters: TR/TE = 1900/2.52 ms, voxel size = 1× 1× 1 mm, flip angle 9°, and field of view = 256 × 192 mm.

To obtain task-related functional MRI (fMRI) images, single shot echo-planar imaging parameters were set at TR/TE = 2500/25 ms, 30 axial slices, voxel size = 3 × 3 × 4 mm, 1-mm interslice gap, flip angle 90°, matrix size = 64 × 64, and field of view = 192 × 192 mm. In each session, the first 5 of 137 scanning images were excluded from analysis.

fMRI data analysis

Functional brain imaging data were analyzed using SPM8 (Wellcome Department of Imaging Neuroscience, http://www.fil.ion.ucl.ac.uk/spm/software/spm8/). For each image, motion and slice-timing correction as well as co-registration into an MPRAGE structural image was performed. The Montreal Neurological Institute (MNI) template was used for spatial normalization, and smoothing was performed using an 8-mm full width half maximum Gaussian kernel. MRI time-series data that contained three-dimensional blood-oxygenation-level-dependent (BOLD) signals of each participant were analyzed using the first-level fixed effects model with general linear model regression analysis. Using the canonical hemodynamic response function implemented in SPM8, a hypothetical hemodynamic time course corresponding to the stimulus presentations under each face-viewing task condition was developed by convolving the hemodynamic response function. Incorporated into the design matrix were 13 hemodynamic models of time series corresponding to the following: i) 6 conditions [3 categories of emotions (happy, fear, and neutral) × 2 types of image presentation (conscious and non-conscious)], ii) target image presentation, and iii) 6 head motions as regressors. Actual BOLD signals were analyzed voxel by voxel using the general linear model (GLM), and during presentation of either a fearful or neutral facial image the parameter estimate for each regressor was calculated and a beta image was generated. Significance was set at $p < 0.001$ (a cluster of > 5 voxels). Also, we took a region of interest (ROI) approach where we searched for significant clusters that survived multiple comparison correction with family-wise error (FWE) within the amygdala mask based on Anatomical Automatic Labeling (AAL) ($p < 0.05$, small volume correction [22]). The random-effects model was used to analyze between-subjects variability. A paired t-test was performed to calculate the t-value for the first t-level contrast value between each SC and SD session. Beta images for the presentation of nonconscious fearful, nonconscious neutral, and each fear-neutral contrast image were used in this analysis.

The t-test revealed no significant difference in amygdala activity during nonconscious face-viewing tasks between the SC and SD conditions (peak MNI coordinate, left amygdala: $x = -14$, $y = -10$, $z = -18$, $t(10) = -1.93$; right amygdala: $x = 18$, $y = -8$, $z = -12$, $t(10) = -2.51$).

Correlation analysis with subjective sleepiness

To investigate whether sleepiness modulates implicit emotional processing, we correlated brain activity during presentation of fearful and neutral facial images with sleepiness during the task in SD and SC sessions. Significance was set at $p < 0.001$ (a cluster of > 5 voxels). We searched for significant clusters that survived multiple comparison correction with FWE within the amygdala mask based on AAL ($p < 0.05$, small volume correction [22]). Beta images for the presentation of nonconscious fearful, nonconscious neutral, and each fear-neutral contrast image were used in this analysis.

Functional connectivity between the amygdala and superior colliculus

To determine whether the amygdala is functionally connected to remote regions and whether changes in this connectivity are related to changes in subjective sleepiness, we conducted functional connectivity analysis, seeded in the clusters in the bilateral amygdala that we obtained from results of the fear-neutral contrast. Because we were particularly interested in the subliminal visual pathway based on a previous study [1], we placed the target ROI in the superior colliculus as this region transmits visual information to the amygdala directly. Using WFU PickAtlas software from the SPM Toolbox, a mask for the superior colliculus was generated based on peak coordinates from results of the previous study.

Functional connectivity between the amygdala and superior colliculus ($Fc_{AMG\text{-}SCo}$) was calculated using CONN toolbox version 13.1 (Alfonso Nieto-Castanon, http://www.alfnie.com/software/conn). Voxel-by-voxel GLM analyses were conducted, with the regression of time-series data in each voxel within the target ROI (superior colliculus) on the time-series data in the seed region. Head motions and hypothetical hemodynamic response to the main event (confounding effects of stimulus-locked transients [23]) were used as regressors. Bandpass-filter range was set at 0.008-0.09 Hz. Individual GLM analyses produced individual estimation maps (beta-maps) for the two sleep conditions (SD or SC) and the two kinds of facial presentation (nonconscious fearful or nonconscious neutral). We first checked the existence of statistically significant FcAMG-SCo during observation of fearful and neutral faces separately using t-tests, and also checked the differential FcAMG-SCo between fearful and neutral faces. Next, the individual beta maps in each facial condition were fed into the correlation analysis with the sleepiness at the time when the data were obtained.

Results were considered significant if p was less than 0.001 and the number of continuous voxels forming a cluster was greater than 5. Furthermore, we searched for significant clusters that survived multiple comparison correction with FWE within the superior colliculus mask ($p < 0.05$, small volume correction [22]).

Increased sleepiness by sleep deprivation and changes in amygdala activity and functional connectivity to the superior colliculus

Next, we examined whether an increase in sleepiness by sleep deprivation promotes changes in amygdala activity and/or functional connectivity between the amygdala and superior colliculus ($Fc_{AMG\text{-}SCo}$). We first calculated individual differential sleepiness between two different sleep states (SD vs. SC) and differential amygdala activation and differential $Fc_{AMG\text{-}SCo}$ between the unconscious fear and neutral faces. We then evaluated the correlation of individual differential sleepiness with differential amygdala activation and differential $Fc_{AMG\text{-}SCo}$. We searched for clusters in the bilateral amygdala whose activity (in response to fear vs. neutral faces) was correlated with sleepiness, and for clusters in the superior colliculus that showed significant functional connectivity to the amygdala during observation of fearful faces. MarsBar software (Matthew Brett, http://marsbar.sourceforge.net /marsbar.pdf) was used to calculate mean contrast values in each cluster.

Statistics

SPSS PASW Statistics 18 software was used for statistical analysis. Behavioral indicators between SD and SC sessions were analyzed using the two-tailed t-test. Results are expressed as mean ± standard deviation. Between-subjects analysis was performed by calculating Pearson's product moment correlation coefficient. Except for the analysis of functional brain activity, data were considered significant at $p < 0.05$.

Results

Sleep-time regulation

From the actigraph data, mean sleep time over the entire 5-day period in the SC and SD sessions was 8.13 ± 0.29 h (8 h 8 min ± 17 min) and 4.67 ± 0.56 h (4 h 40 min ± 34 min), with significantly fewer sleep hours (3.47 ± 0.61 h, or 3 h 28 min ± 37 min) in the SD session ($t(10) = 19.00$, $p < 0.001$).

Subjective sleepiness

Subjective sleepiness scores for the SD session were significantly higher than those for the SC session (SC = 1.63 ± 0.84, SD = 2.5 ± 0.87, $t(10) = 2.932$, $p < 0.05$).

Subjective awareness of masked images

No significant session-related differences were seen in either subjective awareness score (SC = 2.23 ± 0.52, SD = 1.95 ± 0.47, $t(10) = 1.604$).

Button response

No significant session-related differences were seen in either the number or mean time of responses (SC = 2.23 ± 0.52, SD = 1.95 ± 0.47, $t(10) = 1.604$; SC = 11.63 ± 0.6, SD = 11.38 ± 1.16, $t(10) = 0.71$; SC = 596.98 ± 0.153.43, SD = 608.28 ± 115.34, $t(10) = 0.11$, respectively).

fMRI data

fMRI data are shown in Figure 2. Correlation analysis of fear contrasts showed a significant positive correlation between subjective sleepiness and activity in the amygdala, ventromedial prefrontal cortex, hippocampus, and insular cortex [peak MNI coordinates, left amygdala: $x = -30$,

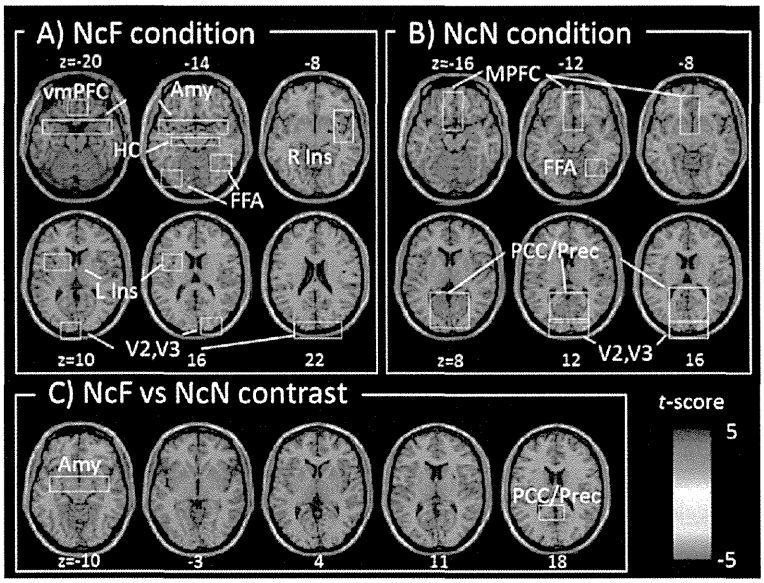

Figure 2 Correlation analysis of the correlation with subjective sleepiness. A)–C) Statistical parametric mapping of different brain regions showing a significant correlation with subjective sleepiness during a face-viewing task: **A)** nonconscious + fear contrasts, **B)** nonconscious + neutral contrasts, and **C)** nonconscious + fear vs. neutral contrasts. Red and blue areas show a significant positive and negative correlation with subjective sleepiness, respectively. **A)** In the nonconscious + fear contrasts, a significant positive correlation is observed in the bilateral amygdala, hippocampus, insula, and ventromedial prefrontal cortex, whereas a significant negative correlation is observed in the secondary and tertiary visual areas and the fusiform face area. **B)** In the nonconscious + neutral contrasts, a significant positive correlation is observed in the ventromedial prefrontal cortex, posterior cingulate cortex, and precuneus, whereas a significant negative correlation is observed in the secondary and tertiary visual areas and the fusiform face area. **C)** In the nonconscious + fear vs. neutral contrasts, the bilateral amygdala and posterior cingulate cortex show a significant positive and negative correlation, respectively. Abbreviations: NcF = Nonconscious fear condition; NcN = Nonconscious neutral condition; Amy = Amygdala; HC = Hippocampus; vMPFC = ventromedial prefrontal cortex; MPFC = medial prefrontal cortex; R Ins = Right Insula; L Ins = Left Insula; FFA = Fusiform face area; PCC = Posterior cingulate cortex; Prec = Precuneus; $p < 0.001$ uncorrected, cluster $k > 5$-voxel threshold; Degrees of freedom (df) = 20.

$y = 0$, $z = -14$, $t(20) = 5.92$, $p < 0.05$ small volume correction with FWE; right amygdala: $x = 28$, $y = 0$, $z = -16$, $t(20) = 4.53$, $p < 0.05$ small volume correction with FWE; ventromedial prefrontal cortex: $x = 2$, $y = 34$, $z = -20$, $t(20) = 4.48$; right hippocampus: $x = 22$, $y = -14$, $z = -16$, $t(20) = 4.18$; left hippocampus: $x = -28$, $y = -22$, $z = -16$, $t(20) = 3.94$; left insular cortex: $x = -30$, $y = 4$, $z = 14$, $t(20) = 7.62$; right insular cortex: $x = 32$, $y = 8$, $z = 12$, $t(20) = 4.37$ (Figure 2A)]. Also, as with the presentation of neutral facial images, subjective sleepiness was significantly negatively correlated with activity in the secondary and tertiary visual cortices and the fusiform face area (FFA) [left visual cortex: $x = -16$, $y = -98$, $z = 24$, $t(20) = 4.61$; right visual cortex: $x = 24$, $y = -96$, $z = 22$, $t(20) = 5.13$; left FFA: $x = -40$, $y = -46$, $z = -10$, $t(20) = 4.41$; right FFA: $x = 40$, $y = -54$, $z = -12$, $t(20) = 5.15$ (Figure 2A)].

On the other hand, correlation analysis of neutral contrasts revealed that subjective sleepiness was significantly positively correlated with activity in the default mode network (DMN) area (i.e., the precuneus, posterior cingulate cortex, inferior parietal gyrus, and medial prefrontal cortex [24,25]) [precuneus: $x = -4$, $y = -72$, $z = 28$, $t(20) = 6.03$; left inferior parietal gyrus: $x = -46$, $y = -48$, $z = 26$, $t(20) = 4.23$; posterior cingulate cortex: $x = -6$, $y = -24$, $z = 32$, $t(20) = 3.71$; medial prefrontal cortex: $x = 4$, $y = 56$, $z = 16$, $t(20) = 5.06$ (Figure 2B)]. Furthermore, a significant negative correlation was observed between subjective sleepiness and activity in the secondary and tertiary visual cortices and the fusiform face area [left visual cortex: $x = -10$, $y = -102$, $z = 18$, $t(20) = 4.21$; right visual cortex: $x = 24$, $y = -96$, $z = 22$, $t(20) = 5.95$; right FFA: $x = 38$, $y = -52$, $z = -10$, $t(20) = 3.80$ (Figure 2B)].

Correlation analysis of fear-neutral contrasts showed a significant positive correlation between subjective sleepiness and activity in the bilateral amygdala [left amygdala: $x = -24$, $y = -4$, $z = -8$, $t(20) = 5.05$; right amygdala: $x = 28$, $y = 8$, $z = -12$, $t(20) = 4.20$ (Table 1, Figures 2C, 3), $p < 0.05$ small volume correction with FWE]. Activity in the precuneus, posterior cingulate cortex, and inferior parietal gyrus in the DMN area was significantly negatively correlated with subjective sleepiness [precuneus: $x = -4$, $y = -74$, $z = 50$, $t(20) = 5.31$; posterior cingulate cortex: $x = -6$, $y = -24$, $z = 32$ $t(20) = 4.62$; left inferior parietal gyrus: $x = -40$, $y = -56$, $z = 54$, $t(20) = 5.31$ (Table 1,

Table 1 Coordinates of brain regions showing a significant correlation with subjective sleepiness in the correlation analysis of fear-neutral contrasts ($p < 0.001$, uncorrected, $k > 5$)

	Brain region			BA	MNI			*t*	Cluster *k*
					x	y	z		
Positive correlation									
	Right	Lentiform nucleus/ Parahippocampal gyrus	Putamen/Amygdala		24	−4	−8	5.05	25
	Right	Lentiform nucleus	Putamen		28	4	12	4.9	16
	Left	Parahippocampal gyrus	Amygdala		−24	−8	−12	4.2	17
Negative correlation									
	Left	Inferior parietal lobule		40	−40	−56	54	5.31	45
	Left	Precuneus		7	−4	−74	50	5.31	219
	Right	Superior frontal gyrus		10	22	56	−8	5.18	59
	Left	Fusiform gyrus		20	−40	−32	−22	4.83	26
	Right	Inferior temporal gyrus		20	34	−8	−42	4.78	33
	Left	Cingulate gyrus		23	−6	−24	32	4.62	74
	Left	Cerebellar tonsil			−50	−56	−42	4.22	6
	Left	Paracentral lobule		5	0	−44	62	4.22	55
	Left	Middle temporal gyrus		20	−56	−38	−12	4.09	5
	Right	Precuneus		7	18	−52	52	4.03	8
	Left	Superior frontal gyrus		11	−4	60	−22	4.02	11
	Right	Medial frontal gyrus		10	8	64	2	3.97	7
	Left	Posterior cingulate		29	−8	−44	16	3.96	11
	Left	Middle frontal gyrus		6	−36	−2	46	3.95	10
	Left	Middle frontal gyrus		11	−26	52	−14	3.82	14

The *x*, *y*, and *z* coordinates denote the peak location on the MNI template.
Abbreviations: BA = Brodmann area; MNI = Montreal Neurological Institute template; Cluster $k = p < 0.001$ uncorrected threshold; Degrees of freedom (*df*) = 20.

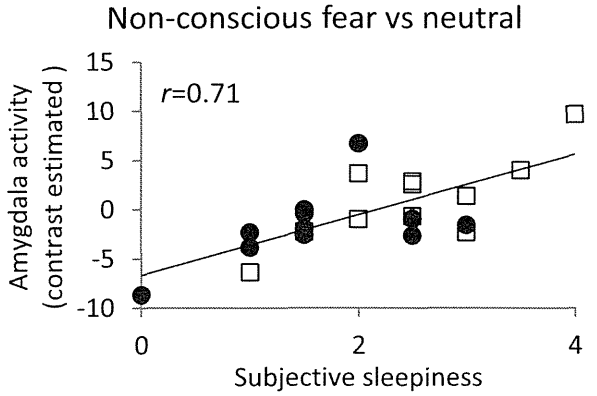

Figure 3 Correlation scatter graph for subjective sleepiness and amygdala activity. In fear-neutral contrasts, amygdala activity is significantly positively correlated with subjective sleepiness during a face-viewing task ($r[20] = 0.71$, $p < 0.001$). Amygdala activity was obtained by averaging clusters in the bilateral amygdala that showed a significant positive correlation in correlation analysis ($p < 0.001$, uncorrected). Data from the SC and SD sessions are shown in different colors in the graph. ●, SC; □, SD. *Abbreviations*: SC = sleep control condition; SD = sleep debt condition; Degrees of freedom (*df*) = 20.

Figure 2C)], presumably reflecting a positive correlation at the time of neutral-face presentation. Subjective sleepiness was not correlated with secondary or tertiary visual areas or the fusiform face area.

Functional connectivity between the amygdala and superior colliculus

We found a significant positive $Fc_{AMG\text{-}SCo}$ during the presentation of fearful faces [peak MNI coordinates (mm) in the superior colliculus: $x = -4$, $y = -26$, $z = -16$, $t(21) = 5.43$, $p < 0.05$ small volume correction with FWE (Figure 4)]. We also found marginally significant $Fc_{AMG\text{-}SCo}$ in the fear-neutral contrast [$x = -4$, $y = -28$, $z = -8$, $t(21) = 3.45$, $p = 0.001$]. On the other hand, no significant connectivity was found during observation of neutral faces [peak MNI coordinates: $x = -4$, $y = -26$, $z = -10$, $t(21) = 1.75$].

We did not find significant a correlation between subjective sleepiness and $Fc_{AMG\text{-}SCo}$ for any type of stimulus [fear: $x = -4$, $y = -32$, $z = -8$, $t(21) = 1.79$; neutral: $x = 0$, $y = -28$, $z = -10$, $t(21) = 2.76$; fear vs. neutral: $x = -6$, $y = -22$, $z = 0$, $t(21) = 2.66$].

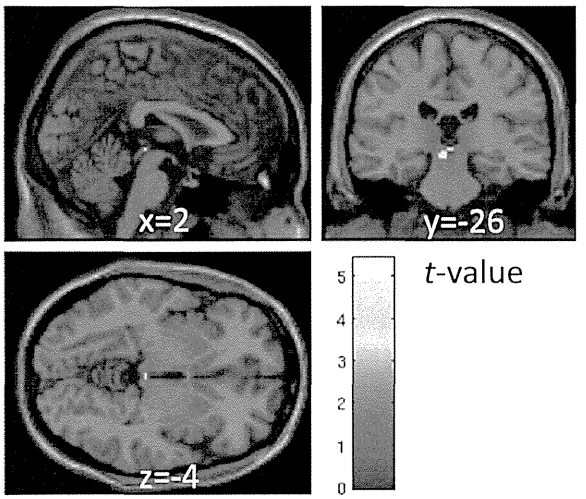

Figure 4 Functional connectivity with the amygdala in fear contrasts. The map shows significant functional connectivity between the bilateral amygdala and other voxels in the brain in both the SC and SD sessions. Significant connectivity was found in the cluster including the superior colliculus, peak MNI coordinate $(x, y, z) = (-4, -26, -10)$ mm, $t(21) = 5.43$, $p = 0.0001$, $k = 26$ contiguous voxels. A significant cluster with a significant connection to the amygdala is rendered on a T1 anatomical referential image displayed by neurological convention, with the left side corresponding to the left hemisphere. MNI, Montreal Neurological Institute template.

Increased sleepiness by sleep deprivation and changes in amygdala activity and functional connectivity to the superior colliculus

After we calculated individual differential amygdala activation, differential $Fc_{AMG\text{-}SCo}$, and differential subjective sleepiness between SD and SC, we obtained cross- correlations between differential amygdala activation, differential $Fc_{AMG\text{-}SCo}$, and differential subjective sleepiness (Figure 5). Differential indices signify changes due to sleep deprivation (SD) compared to the SC session. Changes in amygdala activation and changes in $Fc_{AMG\text{-}SCo}$ by SD were positively correlated with changes in the subjective sleepiness score [$r(10) = 0.66$, $p < 0.05$, $r(10) = 0.70$, $p < 0.05$, respectively (Figure 5)].

Discussion

The results of this study revealed that the subjective feeling of strong sleepiness significantly altered participants' emotional brain reaction toward negative emotional stimuli presented under nonconscious conditions. In particular, the intensity of amygdala activity in response to a fearful expression was significantly positively correlated with subjective sleepiness. On the other hand, in the secondary and tertiary visual areas and the fusiform face area specialized for visual cognition of facial expression [26,27], activity was negatively correlated with subjective sleepiness. We found functional connectivity between the amygdala and superior colliculus ($Fc_{AMG\text{-}SCo}$) during presentation of the fearful face. Further, changes in subjective sleepiness (the difference between the SC and SD sessions) were correlated with both changes in amygdala activity and $Fc_{AMG\text{-}SCo}$ in response to subliminal fearful faces. These findings suggest that an increase in sleepiness enhances subliminal emotion processing that engages the amygdala and its connection to the superior colliculus. They also suggest that an increase in sleepiness enhances amygdala activity and overall subliminal emotion processing via the superior colliculus while at the same time reducing activity in areas involved in visual cognition.

The amygdala is known to play an important role in evoking negative emotional responses [28,29]. Although visual perception of fearful facial expressions leads to amygdala activation in healthy individuals [30], this activation is more pronounced in patients with depression and anxiety disorder [31,32]. On the other hand, when fearful expressions are presented nonconsciously or outside the focus of attention, amygdala activation is similar to that observed under conscious presentation [4,5,33].

The present findings revealed that activation of the amygdala in response to subliminal negative emotional stimuli was augmented by an increase in sleepiness. The

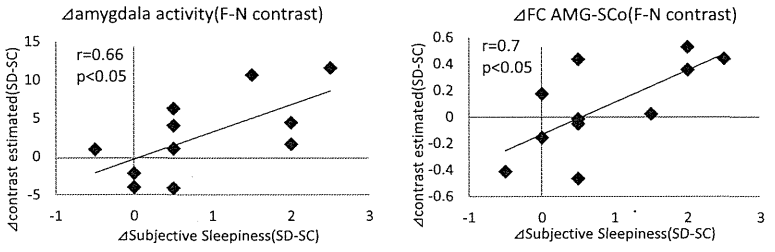

Figure 5 Correlation between intersession differences in amygdala activity, amygdala–superior colliculus functional connectivity, and intersession differences in subjective sleepiness scores. Intersession differences between sleep control and sleep debt sessions of amygdala activity and amygdala-superior colliculus functional connectivity in fear-neutral contrasts correlated positively with intersession differences in subjective scores, $r(10) = 0.66$, $p < 0.05$, $r(10) = 0.70$, $p < 0.05$, respectively. Δvalue, intersession difference between sleep control and sleep debt sessions for each value; SC, sleep control condition; SD, sleep debt condition; $Fc_{AMG\text{-}SCo}$, functional connectivity between amygdala and superior colliculus.

amygdala is neurally connected to brain regions such as the insular cortex, medial prefrontal cortex, and hippocampus, and together they form the brain's emotion network [34-36]. We found that activity of the emotion network in response to a fearful facial expression increased as sleepiness intensified. However, after subtracting the effect of the neutral expression, the amygdala was the only brain region significantly correlated with sleepiness. In other words, during strong sleepiness, the response to negative emotional stimuli was altered most noticeably in the amygdala.

During neutral facial image presentation, subjective sleepiness was significantly positively correlated with activity in the precuneus, posterior cingulate cortex, and medial prefrontal cortex. These regions form the DMN area, which is activated strongly during rest not involving tasks [24,25]. Sleep deprivation was found to enhance activity in the DMN area during a task [14]. In the present study, sleep debt augmented activity in the DMN area during nonconscious presentation of neutral, but not fearful, expressions. Images that remained at the conscious level were neutral facial images under both presentations, suggesting that nonconscious presentation of fearful expressions might enhance attention toward subliminal warnings and prevent the default mode of activity in the DMN area.

Activity in the amygdala increased in participants who experienced intense sleepiness despite reduced responsiveness in the visual area involved in fearful expression. This suggests that subliminal visual signals are transmitted to the amygdala via an alternative pathway that bypasses the visual cortex [3,5,6,11]. In the backward-masking task, a fearful expression was presented for a mere 26 ms without eliciting conscious perception, followed by presentation of a neutral expression long enough (176 ms) to ensure visual cognition. Under mild sleepiness (i.e., highly alert with functional attentional mechanisms), information on neutral facial expression is transmitted to the amygdala via the pathway involved in conscious vision, which might cancel out information from fearful (and fear-neutral) expressions transmitted via the subliminal pathway. When subjects were asked to perform an affect-labeling task to describe the emotion presented in the individual facial stimuli, self-reported distress toward the facial stimuli was reduced compared with the normal viewing task [37], and the activity of amygdala was suppressed [38,39]. Given that the activity in the cortical area involved in visual face recognition was reduced under strong sleepiness in the present study, it is possible that affect labeling of currently presented faces (which remains at the conscious level) is impossible when highly sleepy, exposing the presence and impact of fearful information transmitted via the subliminal pathway.

In this study, nonconscious presentation of fearful facial expressions enhanced the activity of amygdala despite the reduced activity in the cortical area involved in facial recognition. The functional significance of this phenomenon might be that a primitive subliminal hazard perception system was utilized as an alternative mechanism in response to the functional decline in conscious emotion processing. The superior colliculus, which is present in the brain area presumably involved in the subliminal pathway, functions as the center of visual processing in fish and amphibians. On the other hand, the superior colliculus constitutes a small portion of the whole brain in humans, and therefore its function is considered phylogenetically old [40]. In ancient times, fearful facial expressions were important tools for conveying imminent life-threatening danger among tribal members and functioned as basic warning signs among them [41]. It is therefore possible that declines in supraliminal visual cognitive and attentional function due to strong sleepiness evoked strong reactions toward fearful expressions via the phylogenetically old subliminal pathway of emotional processing. It is also possible that the subliminal pathway is involved in the rapid transmission of danger-related information because subliminal information is reportedly transmitted faster than supraliminal information [10]. Furthermore, as shown in this study, activation of subliminal emotional processing due to enhanced sleepiness might also affect emotional adjustment during sleep debt. Although mood decline is likely to occur in response to mild stressors during sleep debt [42], sleep deprivation was reported to increase sensitivity to pleasurable experiences by lowering the threshold value in a task judging valence of pleasure-evoking pictures [43]. A change in nonconscious emotion processing can influence one's conscious state, such as mood, feeling or emotional evaluation [44,45]. Previous studies using nonconscious emotional stimuli have indicated that subjects can be unaware of their own emotional responses [11,46]. According to the somatic marker hypothesis (see [47,48] for details), changes in bodily response such as sympathetic hyperactivity can strongly affect subjective feelings and emotional evaluation without one's conscious awareness of the responses. The amygdala and insula, where activation due to sleepiness was observed in this study, are involved in autonomic nervous system regulation [49,50]. Our findings suggest that the enhancement of subliminal emotional processing during sleep debt might result in involuntary emotional instability, either directly or indirectly (e.g. through change of bodily response), without self-awareness. Because we did not measure sympathetic nervous system indices such as the respiratory and cardiac cycle in this study, we could not confirm that sympathetic activity accompanied enhanced amygdala activity during strong sleepiness. Moreover, the amygdala activation could be explained as the result of increased sympathetic activity due to sleep deprivation. Future studies should ideally measure indices such as

heart rate and respiratory rate in the MRI scanner. In this study, however, the activity of the amygdala was changed by sleepiness only when observing fearful faces, not neutral faces, so a change in the sympathetic system does not completely explain the changes seen in nonconscious emotion responses, although sleepiness should impact subliminal emotional processing and alter amygdala activation.

Conclusion

Sleepiness induced functional decline in brain areas involved in conscious visual cognition of facial expressions, but also enhanced subliminal emotional processing as represented by activity in the amygdala. These findings suggest that an evolutionally old and auxiliary subliminal hazard perception system is activated as a compensatory mechanism when conscious visual cognition is impaired. In addition, enhancement of subliminal emotional processing might cause involuntary emotional instability during sleep debt through changes in emotional response to or evaluation of external stimuli.

Abbreviations

SD: Sleep debt; SC: Sleep control; MRI: Magnetic resonance imaging; fMRI: Functional MRI; MNI: Montreal neurological institute; BOLD: Blood oxygenation level dependent; GLM: General linear model; DMN: Default mode network.

Competing interests

The authors declare that they have no competing interests.

Authors' contributions

YM, SK, KO, YT, YM, and KM designed the study; YM, SK, ME, YK, and AH conducted the sleep restriction experiment; YM, OK, and YT ran the fMRI experiment; YM and YM analyzed the fMRI data; YM, SK, KO, YT, YM, SH, and KM interpreted the data; YM, YM, SH, and KM wrote the manuscript. All authors read and approved the final manuscript.

Acknowledgements

This study was supported by a Grant-in-Aid for the Strategic Research Program for Brain Sciences (Understanding of molecular and environmental bases for brain health) from the Ministry of Education, Culture, Sports, Science and Technology of Japan, an Intramural Research Grant (23–3) for Neurological and Psychiatric Disorders from the National Center of Neurology and Psychiatry, a JSPS KAKENHI (No. 21390335), and a Grant-in-Aid for JSPS Fellows (25–3726).

Author details

[1]Department of Psychophysiology, National Institute of Mental Health, National Center of Neurology and Psychiatry, 4-1-1 Ogawa-Higashi, Kodaira, Tokyo 187-8553, Japan. [2]Graduate School of Integrated Frontier Science, Kyushu University, 6-10-1 Hakozaki, Higashi-ku, Fukuoka 812-8581, Japan. [3]Research Fellow of the Japan Society for the Promotion of Science, 5-3-1, Kojimachi, Chiyoda-ku, Tokyo 102-0082, Japan. [4]Integrative Brain Imaging Center, National Center of Neurology and Psychiatry, 4-1-1 Ogawa-Higashi, Kodaira, Tokyo 187-8553, Japan. [5]Department of Psychology, Keio University, 4-1-1Hiyoshi, Kohoku-ku, Yokohama-shi, Kanagawa 223-8521, Japan. [6]Faculty of Design, Kyushu University 4-9-1 Shiobaru, Minami-ku, Fukuoka 815-8540, Japan.

Received: 1 April 2014 Accepted: 14 August 2014
Published: 19 August 2014

References

1. Williams LM, Das P, Liddell BJ, Kemp AH, Rennie CJ, Gordon E: Mode of functional connectivity in amygdala pathways dissociates level of awareness for signals of fear. *J Neurosci* 2006, 26(36):9264–9271.
2. Morris JS, Ohman A, Dolan RJ: A subcortical pathway to the right amygdala mediating "unseen" fear. *Proc Natl Acad Sci U S A* 1999, 96(4):1680–1685.
3. Liddell BJ, Brown KJ, Kemp AH, Barton MJ, Das P, Peduto A, Gordon E, Williams LM: A direct brainstem-amygdala-cortical 'alarm' system for subliminal signals of fear. *Neuroimage* 2005, 24(1):235–243.
4. Williams MA, Morris AP, McGlone F, Abbott DF, Mattingley JB: Amygdala responses to fearful and happy facial expressions under conditions of binocular suppression. *J Neurosci* 2004, 24(12):2898–2904.
5. Pasley BN, Mayes LC, Schultz RT: Subcortical discrimination of unperceived objects during binocular rivalry. *Neuron* 2004, 42(1):163–172.
6. Tamietto M, Pullens P, de Gelder B, Weiskrantz L, Goebel R: Subcortical connections to human amygdala and changes following destruction of the visual cortex. *Curr Biol* 2012, 22(15):1449–1455.
7. Tamietto M, de Gelder B: Neural bases of the non-conscious perception of emotional signals. *Nat Rev Neurosci* 2010, 11(10):697–709.
8. Pessoa L, Adolphs R: Emotion processing and the amygdala: from a 'low road' to 'many roads' of evaluating biological significance. *Nat Rev Neurosci* 2010, 11(11):773–783.
9. De Gelder B: Uncanny sight in the blind. *Sci Am* 2010, 302(5):60–65.
10. Tamietto M, Castelli L, Vighetti S, Perozzo P, Geminiani G, Weiskrantz L, de Gelder B: Unseen facial and bodily expressions trigger fast emotional reactions. *Proc Natl Acad Sci U S A* 2009, 106(42):17661–17666.
11. Morris JS, DeGelder B, Weiskrantz L, Dolan RJ: Differential extrageniculostriate and amygdala responses to presentation of emotional faces in a cortically blind field. *Brain* 2001, 124(Pt 6):1241–1252.
12. Chuah LY, Chee MW: Functional neuroimaging of sleep deprived healthy volunteers and persons with sleep disorders: a brief review. *Ann Acad Med Singapore* 2008, 37(8):689–694.
13. Chee MW, Chuah LY, Venkatraman V, Chan WY, Philip P, Dinges DF: Functional imaging of working memory following normal sleep and after 24 and 35 h of sleep deprivation: correlations of fronto-parietal activation with performance. *Neuroimage* 2006, 31(1):419–428.
14. Drummond SP, Bischoff-Grethe A, Dinges DF, Ayalon L, Mednick SC, Meloy MJ: The neural basis of the psychomotor vigilance task. *Sleep* 2005, 28(9):1059–1068.
15. Drummond SP, Meloy MJ, Yanagi MA, Orff HJ, Brown GG: Compensatory recruitment after sleep deprivation and the relationship with performance. *Psychiatry Res* 2005, 140(3):211–223.
16. Drummond SP, Brown GG, Salamat JS, Gillin JC: Increasing task difficulty facilitates the cerebral compensatory response to total sleep deprivation. *Sleep* 2004, 27(3):445–451.
17. Swann CE, Yelland GW, Redman JR, Rajaratnam SM: Chronic partial sleep loss increases the facilitatory role of a masked prime in a word recognition task. *J Sleep Res* 2006, 15(1):23–29.
18. Pigarev IN, Fedorov GO, Levichkina EV, Marimon JM, Pigareva ML, Almirall H: Visually triggered K-complexes: a study in New Zealand rabbits. *Exp Brain Res* 2011, 210(1):131–142.
19. Cole RJ, Kripke DF, Gruen W, Mullaney DJ, Gillin JC: Automatic sleep/wake identification from wrist activity. *Sleep* 1992, 15(5):461–469.
20. Ekman P, Friesen WV: Constants across cultures in the face and emotion. *J Pers Soc Psychol* 1971, 17(2):124–129.
21. Ogawa T, Oda M, Yoshikawa S, Akamatsu S: Evaluation of facial expressions differing in face angles : constructing a database of facial expressions. *The Technical Report of the Institute of Electronics, Information and Communication Engineers (HIP, Human Information Processing)* 1997, 97(388):47–52.
22. Worsley KJ, Marrett S, Neelin P, Vandal AC, Friston KJ, Evans AC: A unified statistical approach for determining significant signals in images of cerebral activation. *Hum Brain Mapp* 1996, 4(1):58–73.
23. Friston KJ, Buechel C, Fink GR, Morris J, Rolls E, Dolan RJ: Psychophysiological and modulatory interactions in neuroimaging. *Neuroimage* 1997, 6(3):218–229.
24. Gusnard DA, Raichle ME: Searching for a baseline: functional imaging and the resting human brain. *Nat Rev Neurosci* 2001, 2(10):685–694.
25. Fox MD, Raichle ME: Spontaneous fluctuations in brain activity observed with functional magnetic resonance imaging. *Nat Rev Neurosci* 2007, 8(9):700–711.

26. Vuilleumier P, Pourtois G: **Distributed and interactive brain mechanisms during emotion face perception: evidence from functional neuroimaging.** *Neuropsychologia* 2007, **45**(1):174–194.
27. Fusar-Poli P, Placentino A, Carletti F, Landi P, Allen P, Surguladze S, Benedetti F, Abbamonte M, Gasparotti R, Barale F, Perez J, McGuire P, Politi P: **Functional atlas of emotional faces processing: a voxel-based meta-analysis of 105 functional magnetic resonance imaging studies.** *J Psychiatry Neurosci* 2009, **34**(6):418–432.
28. Halgren E, Walter RD, Cherlow DG, Crandall PH: **Mental phenomena evoked by electrical stimulation of the human hippocampal formation and amygdala.** *Brain* 1978, **101**(1):83–117.
29. Gloor P, Olivier A, Quesney LF, Andermann F, Horowitz S: **The role of the limbic system in experiential phenomena of temporal lobe epilepsy.** *Ann Neurol* 1982, **12**(2):129–144.
30. Fitzgerald DA, Angstadt M, Jelsone LM, Nathan PJ, Phan KL: **Beyond threat: amygdala reactivity across multiple expressions of facial affect.** *Neuroimage* 2006, **30**(4):1441–1448.
31. Dannlowski U, Ohrmann P, Bauer J, Kugel H, Baune BT, Hohoff C, Kersting A, Arolt V, Heindel W, Deckert J, Suslow T: **Serotonergic genes modulate amygdala activity in major depression.** *Genes Brain Behav* 2007, **6**(7):672–676.
32. McClure EB, Monk CS, Nelson EE, Parrish JM, Adler A, Blair RJ, Fromm S, Charney DS, Leibenluft E, Ernst M, Pine DS: **Abnormal attention modulation of fear circuit function in pediatric generalized anxiety disorder.** *Arch Gen Psychiatry* 2007, **64**(1):97–106.
33. Williams LM, Liddell BJ, Kemp AH, Bryant RA, Meares RA, Peduto AS, Gordon E: **Amygdala-prefrontal dissociation of subliminal and supraliminal fear.** *Hum Brain Mapp* 2006, **27**(8):652–661.
34. Phelps EA: **Emotion and cognition: insights from studies of the human amygdala.** *Annu Rev Psychol* 2006, **57**:27–53.
35. Kim MJ, Loucks RA, Palmer AL, Brown AC, Solomon KM, Marchante AN, Whalen PJ: **The structural and functional connectivity of the amygdala: from normal emotion to pathological anxiety.** *Behav Brain Res* 2011, **223**(2):403–410.
36. Craig AD: **How do you feel–now? The anterior insula and human awareness.** *Nat Rev Neurosci* 2009, **10**(1):59–70.
37. Lieberman MD, Inagaki TK, Tabibnia G, Crockett MJ: **Subjective responses to emotional stimuli during labeling, reappraisal, and distraction.** *Emotion* 2011, **11**(3):468–480.
38. Creswell JD, Way BM, Eisenberger NI, Lieberman MD: **Neural correlates of dispositional mindfulness during affect labeling.** *Psychosom Med* 2007, **69**(6):560–565.
39. Hariri AR, Bookheimer SY, Mazziotta JC: **Modulating emotional responses: effects of a neocortical network on the limbic system.** *Neuroreport* 2000, **11**(1):43–48.
40. Northcutt RG: **Understanding vertebrate brain evolution.** *Integr Comp Biol* 2002, **42**(4):743–756.
41. Ekman P: *Emotion in the Human Face.* 2nd edition. Cambridge Cambridgeshire; New York: Cambridge University Press; Editions de la Maison des Sciences de l'Homme; 1982.
42. Minkel JD, Banks S, Htaik O, Moreta MC, Jones CW, McGlinchey EL, Simpson NS, Dinges DF: **Sleep deprivation and stressors: evidence for elevated negative affect in response to mild stressors when sleep deprived.** *Emotion* 2012, **12**(5):1015–1020.
43. Gujar N, Yoo SS, Hu P, Walker MP: **Sleep deprivation amplifies reactivity of brain reward networks, biasing the appraisal of positive emotional experiences.** *J Neurosci* 2011, **31**(12):4466–4474.
44. Tsuchiya N, Adolphs R: **Emotion and consciousness.** *Trends Cogn Sci* 2007, **11**(4):158–167.
45. Prochnow D, Kossack H, Brunheim S, Muller K, Wittsack HJ, Markowitsch HJ, Seitz RJ: **Processing of subliminal facial expressions of emotion: a behavioral and fMRI study.** *Soc Neurosci* 2013, **8**(5):448–461.
46. Dimberg U, Thunberg M, Elmehed K: **Unconscious facial reactions to emotional facial expressions.** *Psychol Sci* 2000, **11**(1):86–89.
47. Bechara A, Damasio H, Tranel D, Damasio AR: **The Iowa Gambling Task and the somatic marker hypothesis: some questions and answers.** *Trends Cogn Sci* 2005, **9**(4):159–162. discussion 162–154.
48. Damasio AR: **The somatic marker hypothesis and the possible functions of the prefrontal cortex.** *Philos Trans R Soc Lond B Biol Sci* 1996, **351**(1346):1413–1420.
49. Kimmerly DS, O'Leary DD, Menon RS, Gati JS, Shoemaker JK: **Cortical regions associated with autonomic cardiovascular regulation during lower body negative pressure in humans.** *J Physiol* 2005, **569**(Pt 1):331–345.
50. Critchley HD: **Psychophysiology of neural, cognitive and affective integration: fMRI and autonomic indicants.** *Int J Psychophysiol* 2009, **73**(2):88–94.

doi:10.1186/1471-2202-15-97
Cite this article as: Motomura *et al.*: Sleepiness induced by sleep-debt enhanced amygdala activity for subliminal signals of fear. *BMC Neuroscience* 2014 15:97.

Lee et al. Journal of Physiological Anthropology 2014, 33:9
http://www.jphysiolanthropol.com/content/33/1/9

Journal of PHYSIOLOGICAL ANTHROPOLOGY

ORIGINAL ARTICLE Open Access

Association between the melanopsin gene polymorphism *OPN4*Ile394Thr* and sleep/wake timing in Japanese university students

Sang-il Lee[1], Akiko Hida[2], Shingo Kitamura[2], Kazuo Mishima[2] and Shigekazu Higuchi[1*]

Abstract

Background: In our previous studies, we found that the Ile394Thr SNP in the melanopsin gene (*OPN4*) was functionally associated with the pupillary light reflex. This indicates the possibility that *OPN4*Ile394Thr* is associated with other non-image forming responses. The aim of this study was therefore to determine whether *OPN4*Ile394Thr* is associated with sleep/wake timing.

Methods: A total of 348 healthy Japanese university students participated in this study. Scalp hair was used to genotype the Ile394Thr SNP of *OPN4*. Sleep habits, including bedtime, wake time and sleep duration, were assessed separately for weekdays and weekends. A total of 328 samples, including 223 samples with TT genotype, 91 with TC genotype and 14 with CC genotype, were used for statistical analysis. No significant difference in age or male/female distribution was found among the three genotype groups.

Results: There was no significant difference in circadian preference among the genotype groups. During weekdays, bedtime, wake time and midpoint of sleep for CC subjects were significantly later than those for TT and TC subjects. However, there was no difference between TT and TC subjects in any of their sleep habits. During weekends, bedtime of CC subjects was significantly later than those of TT and TC subjects, and the midpoint of sleep of CC subjects was significantly later than that of TC subjects.

Conclusions: Our findings demonstrated that *OPN4*Ile394Thr* is associated with sleep/wake timing. We also found that the sleep/wake timing of subjects with the CC genotype was later than that of subjects with the TT or TC genotype.

Keywords: Genotype, Human, Melanopsin gene (*OPN4*), Single nucleotide polymorphism (SNP), Non-image forming responses, Sleep

Background

Melanopsin, a photopigment contained in a small subset of retinal ganglion cells, plays an important role in non-image forming (NIF) responses, including circadian photoentrainment [1], melatonin suppression [2], pupillary light reflex [3,4], sleep behavior [5,6] and alertness [7,8], by transmitting photic irradiance information to the brain. Parallel studies using genetic ablation of melanopsin (*Opn4*) in mice [1,9], using a silent-substitution method in humans [4], and using blind subjects [10,11] have demonstrated that the contribution of melanopsin to NIF responses is as important as, or even more important than, that of the classical photoreceptors (rods and cones).

In our previous studies, we found that the Ile394Thr SNP (rs1079610) in the melanopsin gene (*OPN4*) was functionally associated with pupillary light reflex (PLR) and that subjects with different genotypes of Ile394Thr SNP showed different degrees of responsiveness to light [12,13]. Thus, *OPN4*Ile394Thr* might be a factor involved in inter-individual differences in other NIF responses depending on light, such as circadian phase-shifting, but this remains unclear.

The endogenous circadian clock in mammals is a self-sustained oscillation with a period of about 24 hours. In fact, the circadian clock runs free without entrainment (synchronization) to environmental signals, especially the

* Correspondence: higu-s@design.kyushu-u.ac.jp
[1]Department of Human Science, Faculty of Design, Kyushu University, 4-9-1 Shiobaru, Minami-ku, Fukuoka 815-8540, Japan
Full list of author information is available at the end of the article

light/dark cycle in a day. As mentioned above, parallel studies have demonstrated an important role of melanopsin in circadian entrainment [1,5,11,14]. Melanopsin-containing retinal ganglion cells detect irradiance information and transmit the photic signal to the suprachiasmatic nucleus, the circadian pacemaker, located in the hypothalamus [15].

An individual circadian phase shows a light intensity-dependent manner and can be advanced or delayed depending on exposure timing to light. Notably, Zeitzer *et al.* [16] found that phase-delaying effects of light were increased in humans during early night and that the delayed phase appeared with exposure to not only bright light but also low irradiance light. It is therefore possible that the different degrees of responsiveness to light among *OPN4*Ile394Thr* genotypes may influence circadian phase.

Sleep/wake timing in humans is thought to reflect circadian phase [17,18] and to be correlated with dim light melatonin onset (DLMO) phase, which has been used to estimate an individual's circadian phase [19,20]. Aoki *et al.* [21] found that the magnitude of light-induced melatonin suppression in patients with DSPS (delayed sleep phase syndrome) was greater than that in normal subjects. This indicates the possibility that inter-individual differences in circadian phase are associated with photoreceptor light sensitivity.

Taken together, we hypothesized that the effect of Ile394Thr SNP on circadian phase is reflected in sleep/wake timing. Hence, the aim of this study was to determine whether *OPN4*Ile394Thr* is associated with sleep/wake timing.

Methods

Subjects

A total of 348 healthy Japanese university students (mean age: 20.9 years; SD: 2.2) with common color vision (Ishihara color-blindness test) participated in this study. Exclusion criteria included medication or drug consumption and shift work. All participants were enrolled with written consent of each participant, and the study was approved by the Ethical Committee of Kyushu University and the Ethics committee of the National Center of Neurology and Psychiatry. There was no significant difference in age or male/female distribution among the three genotype groups. Table 1 shows the demographical characteristics of the subjects.

Investigation of circadian preference and sleep-wake timing

So-called morningness-eveningness, namely circadian preference, is an individual characteristic and shows a strong correlation with sleep/wake timing [22]. A Japanese version of the Morningness-Eveningness Questionnaire (MEQ) [23] was used to evaluate the effect of individual circadian preference on sleep/wake timing. In addition, sleep habits (bedtime, wake time and sleep duration) were assessed separately for weekdays and weekends, because individual sleep/wake times have been shown to differ greatly between weekdays and weekends [24]. Besides sleep/wake timing, midpoint of sleep has also been used to estimate an individual's circadian phase, and it has been shown to have a strong correlation with DLMO phase [25,26]. The midpoint of sleep was calculated on the basis of self-reported bedtime and wake time.

Table 1 Demographical characteristics of each genotype group

Genotype	TT	TC	CC	*P*-value
n	223	91	14	
Sex (M:F)	122:101	49:42	4:10	0.163 (χ^2)
Age (years ± SD)	21.0 ± 2.3	20.8 ± 2.0	21.3 ± 1.5	0.667

Genotyping

Genomic DNA samples were extracted from a scalp hair using an FM Kit (Wako Pure Chemical Industries, Ltd., Osaka, Japan), and Ile394Thr SNP was genotyped in all participants by using TaqMan SNP genotyping assays (Applied Biosystems, Foster City, California, USA). The genotype groups were classified as TT, TC and CC, and the numbers of subjects in those groups were 232, 94 and 14, respectively (eight being undetermined). Genotype frequency of *OPN4*Ile394Thr* was consistent with the Hardy-Weinberg equilibrium ($\chi^2 = 2.12$, ns), and the T and C allele frequencies of Ile394Thr SNP were 82.1% and 17.9%, respectively.

Statistical analysis

Subjects who did not complete the self-assessment questionnaire were excluded. After exclusion, a total of 328 samples, including 223 samples with TT genotype (122 men and 101 women; 21.0 ± 2.3 years old), 91 samples with TC genotype (49 men and 42 women, 20.8 ± 2.0 years old) and 14 samples with CC genotype (4 men and 10 women, 21.3 ± 1.5 years old), were used for statistical analysis (Table 1).

To evaluate the differences among the genotype groups for dependent variables, including sleep habits and circadian preference, we used one-way multivariate ANOVA (IBM© SPSS© version 21, New York, USA) with the genotypes as independent variables. Tukey (honestly significant difference) HSD *post hoc* tests were carried out when the interaction between genotypes and each dependent variable was significant. $P < 0.05$ was considered to be statistically significant.

Results

The MEQ mean scores and standard deviations were 48.4 ± 7.4 in the TT subjects, 48.6 ± 7.3 in the TC subjects and

44.8 ± 6.6 in the CC subjects (Table 1). ANOVA showed no significant difference among *OPN4*Ile394Thr* genotypes.

ANOVA for the data during weekdays showed main effects of genotype on bedtime ($F = 7.058$; $P < 0.01$), wake time ($F = 3.353$; $P < 0.05$) and midpoint of sleep ($F = 5.622$; $P < 0.01$). No significant effect of genotype on sleep duration was found. In the sleep habits during weekends, main effects of genotype were found on bedtime ($F = 5.624$; $P < 0.01$) and midpoint of sleep ($F = 3.964$; $P < 0.05$) but not on wake time or sleep duration (Table 2).

Figure 1 shows bedtime and wake time of each genotype group both on weekdays and weekends. During weekdays, CC subjects reported significantly later bedtimes than those of TT subjects and TC subjects as well as later wake times. During weekends, CC subjects showed later bedtime than those for TT subjects and TC subjects, while there was no significant difference among the genotype groups in wake time. No significant difference was found between TT and TC subjects in any of the sleep habits.

The midpoint of sleep for CC subjects was significantly later than those for the TT subjects and TC subjects on weekdays, but no significant difference was found between TT subjects and TC subjects. The midpoint of sleep for the CC subjects was later than that for the TC subjects on weekends, but no significant difference was found between TT subjects and CC subjects or between TC subjects and TT subjects (Figure 2).

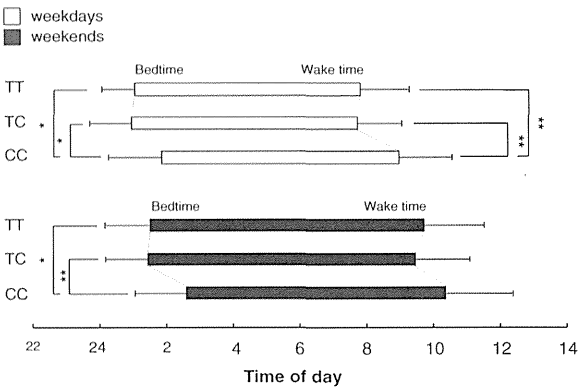

Figure 1 Comparison of bedtime and wake time (mean + SD) among TT (n = 223), TC (n = 91) and CC (n = 14) subjects during weekdays (white bars) and weekends (black bars). During weekdays, both the bedtime and wake time of CC subjects were significantly later than those of TT and TC subjects. During weekends, the results for bedtime were consistent with those during weekdays, but there were no significant differences among genotype groups in wake time. *$P < 0.05$, **$P < 0.01$.

Discussion

We attempted to determine the association between *OPN4*Ile394Thr* and sleep habits. We found that subjects with the CC genotype had later sleep/wake timing and later midpoint of sleep than those for subjects with the TT or TC genotype, indicating that *OPN4*Ile394Thr* is associated with sleep/wake timing. On the other hand, the circadian preferences identified by MEQ scores showed similar trends among the genotype groups, indicating that the sleep habits of subjects with each genotype were not biased by individual preference.

Light is a critical environmental cue for circadian entrainment and circadian phase can be advanced or delayed depending on light intensity and exposure timing. Exposure to light at night results in phase delay. In support of this, it has been reported that exposure of human subjects to ordinary room light with low irradiance (approximately 300 lux) during the night caused delayed circadian phase [16,27], melatonin suppression [28], and

Table 2 Morningness-Eveningness Questionnaire (MEQ) score and sleep habits of each genotype group

Genotype	TT (n = 223)	TC (n = 91)	CC (n = 14)
MEQ score	48.4 ± 7.4	48.6 ± 7.3	44.8 ± 6.6
Weekdays			
Bedtime	1:03 ± 0:59	0:58 ± 1:14	1:52 ± 1:36
Wake time	7:49 ± 1:28	7:44 ± 1:20	8:59 ± 1:35
Mid-sleep	4:26 ± 1:06	8:17 ± 1:07	5:26 ± 1:29
Sleep duration	6:16 ± 1:02	6:25 ± 1:15	6:58 ± 1:20
Weekends			
Bedtime	1:31 ± 1:21	1:26 ± 1:15	2:35 ± 1:31
Wake time	9:44 ± 1:47	9:26 ± 1:38	10:23 ± 2:00
Mid-sleep	5:37 ± 1:24	5:26 ± 1:17	6:29 ± 1:41
Sleep duration	8:08 ± 1:26	8:03 ± 1:41	7:45 ± 1:27

Values indicate means ± SD.

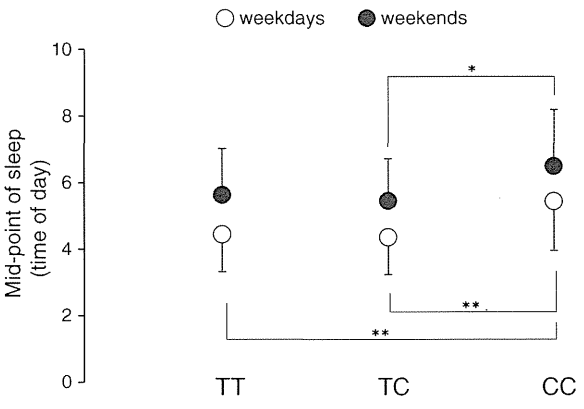

Figure 2 Comparison of midpoint of sleep (mean + SD) among TT (n = 223), TC (n = 91) and CC (n = 14) subjects during weekdays (white circles) and weekends (black circles). During weekdays, the midpoint of sleep of CC subjects was significantly later than those of TT and TC subjects. During weekends, there was a significant difference in midpoint of sleep only between TC and CC subjects. *$P < 0.05$, **$P < 0.01$.

alertness [29]. All of the subjects who participated in the present study were university students and had late bedtimes (mean bedtime: 1:15 AM), which means, although we did not assess light conditions for the subjects in daily life, it can be assumed that the subjects were exposed to indoor light for a long duration during the night. Thus, it is possible that the findings in this study were due to the effect of light exposure at night.

In our previous study, we found that pupilloconstriction of TC and CC subjects or a combined group (TC + CC) was greater than that of TT subjects, suggesting that the genotype with C allele is highly responsive to light [12,13]. Given that the phase-delaying response to light follows a logistic dose–response curve [16], the delayed sleep/wake timing of CC subjects might be a consequence of the high responsiveness to light.

Unlike on weekends, it is difficult for an individual circadian phase, which is strongly affected by social constraints, especially wake time, to be reflected in the sleep/wake cycle on weekdays. Despite this, delayed sleep phase of the CC subjects was observed more clearly during weekdays than during weekends. Although university students are under a time constraint on weekdays, the level of the constraint is weak. In addition, sleep is generated by the interaction between circadian and homeostatic mechanisms, and the latter mechanism is thought to be an increase in sleep pressure during wakefulness and dissipation during subsequent sleep. Particularly in adolescents, sleep debt is likely to accumulate during weekdays and therefore lead to oversleep as a compensation for sleep loss during weekends. Thus, the disappearance of a statistical difference among genotypes in wake time and midpoint of sleep during weekends might be due to homeostatic sleep regulation.

However, the relationship between *OPN4*Ile394Thr* and sleep habits in this study was not consistent with the results for the relationship between *OPN4*Ile394Thr* and PLR in our previous study: sleep/wake timing of the CC subjects was significantly delayed compared to that of the TT and TC subjects, whereas no difference was found between the TC and CC subjects in PLR. It is not clear what caused this, but it indicates that the previous results for PLR cannot sufficiently explain the sleep phase difference among *OPN4*Ile394Thr* genotypes. Compared to PLR, a more complicated mechanism and more factors are involved in sleep. For instance, interindividual differences in endogenous circadian rhythm, circadian phase and sleep timing have been reported [30,31]. Furthermore, contribution of the *CLOCK* gene to circadian phenotypes, particularly sleep timing, has been reported [32,33].

Furthermore, melanopsin has a characteristic spectral sensitivity λ_{max} around 480 nm. The effect of light with a high-color temperature (that is, blue-enriched) on melatonin suppression or sleep has been investigated [34-36]. Also, in our previous study, we found that the difference between *OPN4*Ile394Thr* genotypes in PLR depends on light wavelength: greater differences were observed with a short wavelength light [13]. Therefore, in future work, those factors should be evaluated to validate the findings in this study.

The sample size for CC genotype was small (n = 14) compared to TT and TC subjects. As International HapMap Project reported, the frequency of CC genotype is relatively low not only in Japanese in Tokyo (2.3%) but also in other ethnic groups; for example, 13.3% of Han Chinese in Beijing and 12.3% of European ancestry in Utah state. To enhance confidence in our findings, larger samples will be required.

Perspective

According to the database of International HapMap Project, C allele frequency of Ile394Thr SNP in CEU (European ancestry in Utah state, 34.2%) is larger than that in JPT (Japanese in Tokyo, 17.0%) and that in YRI (Yoruba in Nigeria, 14.2%). It was also found that pupillary light response in CC genotype is larger in the European population [37]. These findings mean that the proportion of people with high sensitivity to light might be relatively large in the European population. It is thought that light skin color in the European population results from genetic adaptation to a short duration of sunlight in a high latitude area. Another example of the health risk of a short duration of sunlight is seasonal affective disorder (SAD), which is involved in the mechanism of melanopsin-containing non-visual response to light. Although it has been reported that melanopsin gene polymorphism is associated with prevalence of SAD [38], it is unknown whether natural selection has driven it or not. Further study based on population genetics, such as a statistical approach to estimate the degree of population differentiation (Wright's Fst) [39] and to measure linkage disequilibrium as evidence of selective sweep [40], is needed.

Although we found an association between *OPN4*Ile394Thr* and sleep timing in this study, an association was not found in another study that was conducted in the USA using middle-aged European subjects [41]. This inconsistency suggests that associations between genotype and phenotypic variations are not simple and that these relations are modulated by environment and age. In the present study, the association between *OPN4* polymorphism and sleep timing was thought to have been due to the effect of light at night on the circadian phase. In Japan, most people are likely to use a fluorescent lamp at home and some tend to use high-color temperature light, which has an impact on sleep and circadian rhythm. In addition, our subjects were university

students, who have been reported to have a tendency to delay sleep timing due to weak social *zeitgebers* [42]. These cultural and environmental factors in Japanese university students might strengthen the association between *OPN4* polymorphism and sleep timing. In physiological anthropology, functional connections and biological significance between genotypic and phenotypic variations should be clarified in terms of interaction of culture and living environments in a targeted population.

Conclusion

Our findings demonstrated that *OPN4*Ile394Thr* is associated with sleep/wake timing. We also found that the sleep/wake timing of subjects with the CC genotype was later than that of subjects with the TT or TC genotype.

Abbreviations

DLMO: dim light melatonin onset; DSPS: delayed sleep phase syndrome; MEQ: Morningness-Eveningness Questionnaire; NIF: non-image forming; PLR: pupillary light reflex; SAD: seasonal affective disorder; SNP: single nucleotide polymorphism.

Competing interests

The authors declare that they have no competing interests.

Authors' contributions

SL collected experimental data, performed statistical analysis and wrote the manuscript. SL and SH participated in the design of the study. SL and AH carried out the molecular genetic analysis. SK, AH and KM revised the manuscript. SH supervised the study and helped to draft the manuscript. All authors read and approved the final manuscript.

Acknowledgements

This study was supported in part by JSPS KAKENHI (24370102) and a part of this study is the result of 'Understanding of Molecular and Environmental Bases for Brain Health' carried out under the Strategic Research Program for Brain Sciences by the Ministry of Education, Culture, Sports, Science and Technology of Japan. The funders had no role in study design, data collection and analysis, decision to publish, or preparation of the manuscript. We would like to thank Takeshi Nishi at Kyushu University, Kaoru Inami at Fukuoka Women's University and especially Mie Kato at National Center of Neurology and Psychiatry for technical assistance in genetic analysis.

Author details

[1]Department of Human Science, Faculty of Design, Kyushu University, 4-9-1 Shiobaru, Minami-ku, Fukuoka 815-8540, Japan. [2]Department of Psychophysiology, National Institute of Mental Health, National Center of Neurology and Psychiatry, 4-1-1 Ogawa-Higashi, Kodaira, Tokyo 187-8553, Japan.

Received: 13 December 2013 Accepted: 25 March 2014
Published: 12 May 2014

References

1. Panda S, Sato TK, Castrucci AM, Rollag MD, DeGrip WJ, Hogenesch JB, Provencio I, Kay SA: **Melanopsin (Opn4) requirement for normal light-induced circadian phase shifting.** *Science* 2002, **298**:2213–2216.
2. Brainard GC, Hanifin JP, Rollag MD, Greeson J, Byrne B, Glickman G, Gerner E, Sanford B: **Human melatonin regulation is not mediated by the three cone photopic visual system.** *J Clin Endocrinol Metab* 2001, **86**:433–436.
3. Gamlin PD, McDougal DH, Pokorny J, Smith VC, Yau KW, Dacey DM: **Human and macaque pupil responses driven by melanopsin-containing retinal ganglion cells.** *Vision Res* 2007, **47**:946–954.
4. Tsujimura S, Ukai K, Ohama D, Nuruki A, Yunokuchi K: **Contribution of human melanopsin retinal ganglion cells to steady-state pupil responses.** *Proc Biol Sci* 2010, **277**:2485–2492.
5. Lupi D, Oster H, Thompson S, Foster RG: **The acute light-induction of sleep is mediated by OPN4-based photoreception.** *Nat Neurosci* 2008, **11**:1068–1073.
6. Tsai JW, Hannibal J, Hagiwara G, Colas D, Ruppert E, Ruby NF, Heller HC, Franken P, Bourgin P: **Melanopsin as a sleep modulator: circadian gating of the direct effects of light on sleep and altered sleep homeostasis in Opn4(−/−) mice.** *Plos Biol* 2009, **7**:e1000125.
7. Cajochen C, Munch M, Kobialka S, Krauchi K, Steiner R, Oelhafen P, Orgul S, Wirz-Justice A: **High sensitivity of human melatonin, alertness, thermoregulation, and heart rate to short wavelength light.** *J Clin Endocrinol Metab* 2005, **90**:1311–1316.
8. An M, Huang J, Shimomura Y, Katsuura T: **Time-of-day-dependent effects of monochromatic light exposure on human cognitive function.** *J Physiol Anthropol* 2009, **28**:217–223.
9. Lucas RJ, Hattar S, Takao M, Berson DM, Foster RG, Yau KW: **Diminished pupillary light reflex at high irradiances in melanopsin-knockout mice.** *Science* 2003, **299**:245–247.
10. Gooley JJ, Mien IH, St Hilaire MA, Yeo SC, Chua ECP, van Reen E, Hanley CJ, Hull JT, Czeisler CA, Lockley SW: **Melanopsin and rod-cone photoreceptors play different roles in mediating pupillary light responses during exposure to continuous light in humans.** *J Neurosci* 2012, **32**:14242–14253.
11. Zaidi FH, Hull JT, Peirson SN, Wulff K, Aeschbach D, Gooley JJ, Brainard GC, Gregory-Evans K, Rizzo JF, Czeisler CA, Foster RG, Moseley MJ, Lockley SW: **Short-wavelength light sensitivity of circadian, pupillary, and visual awareness in humans lacking an outer retina.** *Curr Biol* 2007, **17**:2122–2128.
12. Higuchi S, Hida A, Tsujimura S, Mishima K, Yasukouchi A, Lee SI, Kinjyo Y, Miyahira M: **Melanopsin gene polymorphism *I394T* is associated with pupillary light responses in a dose-dependent manner.** *Plos One* 2013, **8**:e60310.
13. Lee SI, Hida A, Tsujimura S, Morita T, Mishima K, Higuchi S: **Association between melanopsin gene polymorphism (*I394T*) and pupillary light reflex is dependent on light wavelength.** *J Physiol Anthropol* 2013, **32**:16.
14. Altimus CM, Guler AD, Villa KL, McNeill DS, Legates TA, Hattar S: **Rods-cones and melanopsin detect light and dark to modulate sleep independent of image formation.** *Proc Natl Acad Sci U S A* 2008, **105**:19998–20003.
15. Hattar S, Kumar M, Park A, Tong P, Tung J, Yau KW, Berson DM: **Central projections of melanopsin-expressing retinal ganglion cells in the mouse.** *J Comp Neurol* 2006, **497**:326–349.
16. Zeitzer JM, Dijk DJ, Kronauer R, Brown E, Czeisler C: **Sensitivity of the human circadian pacemaker to nocturnal light: melatonin phase resetting and suppression.** *J Physiol* 2000, **526**(Pt 3):695–702.
17. Borbely AA: **A two process model of sleep regulation.** *Human Neurobiol* 1982, **1**:195–204.
18. Dijk DJ, Czeisler CA: **Paradoxical timing of the circadian rhythm of sleep propensity serves to consolidate sleep and wakefulness in humans.** *Neurosci Lett* 1994, **166**:63–68.
19. Burgess HJ, Eastman CI: **The dim light melatonin onset following fixed and free sleep schedules.** *J Sleep Res* 2005, **14**:229–237.
20. Martin SK, Eastman CI: **Sleep logs of young adults with self-selected sleep times predict the dim light melatonin onset.** *Chronobiol Int* 2002, **19**:695–707.
21. Aoki H, Ozeki Y, Yamada N: **Hypersensitivity of melatonin suppression in response to light in patients with delayed sleep phase syndrome.** *Chronobio Int* 2001, **18**:263–271.
22. Mongrain V, Lavoie S, Selmaoui B, Paquet J, Dumont M: **Phase relationships between sleep-wake cycle and underlying circadian rhythms in Morningness-Eveningness.** *J Biol Rhythms* 2004, **19**:248–257.
23. Horne JA, Ostberg O: **A self-assessment questionnaire to determine morningness-eveningness in human circadian rhythms.** *Int J Chronobiol* 1976, **4**:97–110.
24. Roenneberg T, Wirz-Justice A, Merrow M: **Life between clocks: daily temporal patterns of human chronotypes.** *J Biol Rhythms* 2003, **18**:80–90.
25. Crowley SJ, Acebo C, Fallone G, Carskadon MA: **Estimating dim light melatonin onset (DLMO) phase in adolescents using summer or school-year sleep/wake schedules.** *Sleep* 2006, **29**:1632–1641.
26. Terman JS, Terman M, Lo ES, Cooper TB: **Circadian time of morning light administration and therapeutic response in winter depression.** *Arch Gen Psychiatry* 2001, **58**:69–75.
27. Burgess HJ: **Evening ambient light exposure can reduce circadian phase advances to morning light independent of sleep deprivation.** *J Sleep Res* 2013, **22**:83–88.
28. Gooley JJ, Chamberlain K, Smith KA, Khalsa SB, Rajaratnam SM, Van Reen E, Zeitzer JM, Czeisler CA, Lockley SW: **Exposure to room light before**

bedtime suppresses melatonin onset and shortens melatonin duration in humans. *J Clin Endocrinol Metab* 2011, **96**:E463–E472.
29. Cajochen C, Zeitzer JM, Czeisler CA, Dijk DJ: **Dose–response relationship for light intensity and ocular and electroencephalographic correlates of human alertness.** *Behav Brain Res* 2000, **115**:75–83.
30. Duffy JF, Rimmer DW, Czeisler CA: **Association of intrinsic circadian period with morningness-eveningness, usual wake time, and circadian phase.** *Behav Neurosci* 2001, **115**:895–899.
31. Hida A, Kitamura S, Ohsawa Y, Enomoto M, Katayose Y, Motomura Y, Moriguchi Y, Nozaki K, Watanabe M, Aritake S, Higuchi S, Kato M, Kamei Y, Yamazaki S, Goto Y, Ikeda M, Mishima K: ***In vitro*** **circadian period is associated with circadian/sleep preference.** *Sci Rep* 2013, **2074**:3.
32. Ebisawa T, Uchiyama M, Kajimura N, Mishima K, Kamei Y, Katoh M, Watanabe T, Sekimoto M, Shibui K, Kim K, Kudo Y, Ozeki Y, Sugishita M, Toyoshima R, Inoue Y, Yamada N, Nagase T, Ozaki N, Ohara O, Ishida N, Okawa M, Takahashi K, Yamauchi T: **Association of structural polymorphisms in the human *period3* gene with delayed sleep phase syndrome.** *EMBO Rep* 2001, **2**:342–346.
33. Mishima K, Tozawa T, Satoh K, Saitoh H, Mishima Y: **The 3111 T/C polymorphism of *hClock* is associated with evening preference and delayed sleep timing in a Japanese population sample.** *Am J Med Genet B Neuropsychiatr Genet* 2005, **133B**:101–104.
34. Chellappa SL, Steiner R, Blattner P, Oelhafen P, Gotz T, Cajochen C: **Non-visual effects of light on melatonin, alertness and cognitive performance: can blue-enriched light keep us alert?** *Plos One* 2011, **6**:e16429.
35. Kozaki T, Kitamura S, Higashihara Y, Ishibashi K, Noguchi H, Yasukouchi A: **Effect of color temperature of light sources on slow-wave sleep.** *J Physiol Anthropol Appl Human Sci* 2005, **24**:183–186.
36. Santhi N, Thorne HC, van der Veen DR, Johnsen S, Mills SL, Hommes V, Schlangen LJ, Archer SN, Dijk DJ: **The spectral composition of evening light and individual differences in the suppression of melatonin and delay of sleep in humans.** *J Pineal Res* 2012, **53**:47–59.
37. Roecklein K, Wong P, Ernecoff N, Miller M, Donofry S, Kamarck M, Wood-Vasey WM, Franzen P: **The post illumination pupil response is reduced in seasonal affective disorder.** *Psychiatry Res* 2013, **210**:150–158.
38. Roecklein KA, Rohan KJ, Duncan WC, Rollag MD, Rosenthal NE, Lipsky RH, Provencio I: **A missense variant (*P10L*) of the melanopsin (*OPN4*) gene in seasonal affective disorder.** *J Affect Disord* 2009, **114**:279–285.
39. Wright S: *Evolution and the genetics of populations. Vol 2: The theory of gene frequencies.* Chicago: University of Chicago press; 1969.
40. The International HapMap Consortium: **A haplotype map of the human genome.** *Nature* 2005, **437**:1299–1320.
41. Roecklein KA, Wong PM, Franzen PL, Hasler BP, Wood-Vasey WM, Nimgaonkar VL, Miller MA, Kepreos KM, Ferrell RE, Manuck SB: **Melanopsin gene variations interact with season to predict sleep onset and chronotype.** *Chronobiol Int* 2012, **29**:1036–1047.
42. Urner M, Tornic J, Bloch KE: **Sleep patterns in high school and university students: a longitudinal study.** *Chronobiol Int* 2009, **26**:1222–1234.

doi:10.1186/1880-6805-33-9
Cite this article as: Lee *et al.*: Association between the melanopsin gene polymorphism *OPN4*Ile394Thr* and sleep/wake timing in Japanese university students. *Journal of Physiological Anthropology* 2014 **33**:9.

THE JOURNAL OF BIOLOGICAL CHEMISTRY VOL. 289, NO. 15, pp. 10785–10796, April 11, 2014

Defective Craniofacial Development and Brain Function in a Mouse Model for Depletion of Intracellular Inositol Synthesis*[S]

Received for publication, November 20, 2013, and in revised form, February 11, 2014 Published, JBC Papers in Press, February 19, 2014, DOI 10.1074/jbc.M113.536706

Tetsuo Ohnishi[‡1], **Takuya Murata**[§], **Akiko Watanabe**[‡], **Akiko Hida**[¶], **Hisako Ohba**[‡], **Yoshimi Iwayama**[‡], **Kazuo Mishima**[¶], **Yoichi Gondo**[§], **and Takeo Yoshikawa**[‡]

From the [‡]*Laboratory for Molecular Psychiatry, RIKEN Brain Science Institute, Wako, Saitama 351-0198, the* [§]*Mutagenesis and Genomics Team, RIKEN BioResource Center, Tsukuba, Ibaraki 305-0074, and the* [¶]*Department of Psychophysiology, National Institute of Mental Health, National Center of Neurology and Psychiatry, Kodaira, Tokyo 187-8553, Japan*

Background: Lithium exerts a mood-stabilizing effect and inhibits *myo*-inositol monophosphatase (IMPase).
Results: IMPase mutant mice had impaired jaw formation and mimicked lithium-induced behaviors.
Conclusion: Craniofacial development and brain function require intracellular inositol production.
Significance: This mouse model reveals molecular mechanisms relevant to understanding lithium's efficacy and inositol-mediated developmental processes.

myo-Inositol is an essential biomolecule that is synthesized by *myo*-inositol monophosphatase (IMPase) from inositol monophosphate species. The enzymatic activity of IMPase is inhibited by lithium, a drug used for the treatment of mood swings seen in bipolar disorder. Therefore, *myo*-inositol is thought to have an important role in the mechanism of bipolar disorder, although the details remain elusive. We screened an ethyl nitrosourea mutant mouse library for IMPase gene (*Impa*) mutations and identified an *Impa1* T95K missense mutation. The mutant protein possessed undetectable enzymatic activity. Homozygotes died perinatally, and E18.5 embryos exhibited striking developmental defects, including hypoplasia of the mandible and asymmetric fusion of ribs to the sternum. Perinatal lethality and morphological defects in homozygotes were rescued by dietary *myo*-inositol. Rescued homozygotes raised on normal drinking water after weaning exhibited a hyper-locomotive trait and prolonged circadian periods, as reported in rodents treated with lithium. Our mice should be advantageous, compared with those generated by the conventional gene knock-out strategy, because they carry minimal genomic damage, *e.g.* a point mutation. In conclusion, our results reveal critical roles for intracellular *myo*-inositol synthesis in craniofacial development and the maintenance of proper brain function. Furthermore, this mouse model for cellular inositol depletion could be beneficial for understanding the molecular mechanisms underlying the clinical effect of lithium and *myo*-inositol-mediated skeletal development.

Lithium salts are used as a first-line drug to treat psychiatric illnesses, particularly bipolar (manic depressive) disorder. Evidence indicates that the mood-stabilizing action of lithium is mediated by inhibiting *myo*-inositol monophosphatase (IMPase,[2] EC 3.1.3.25) activity, thereby inducing intracellular inositol depletion (1–3). IMPase generates *myo*-inositol, a substrate for the membrane phospholipid phosphatidylinositol, from inositol monophosphate species, which are produced in cells by the multistep dephosphorylation of higher inositol phosphates ("recycling" of inositol) or by the isomerization of D-glucose 6-phosphate ("*de novo* synthesis" of inositol). Mammalian cells express IMPase 1 and IMPase 2, which are encoded by *Impa1/IMPA* (4, 5) and *Impa2/IMPA2* (6, 7), respectively. Their primary structures are closely related to each other, whereas their three-dimensional structures and enzymatic characteristics vary slightly but significantly (8–10). Importantly, IMPase 1 is more sensitive to lithium inhibition than IMPase 2 in our *in vitro* assay. This finding strengthens the importance of IMPase 1 as a *bona fide* target for lithium therapy. However, genetic variations in *IMPA2*, but not in *IMPA1*, have been implicated in multiple neuropsychiatric diseases, including schizophrenia (11), bipolar disorder (12, 13), and febrile seizures (14), suggesting a role for the *IMPA2* gene in the genetic risk for these illnesses. Although these lines of evidence support critical roles for IMPase and *myo*-inositol in maintaining normal brain function, it still remains unclear whether and how inositol depletion mediates the therapeutic efficacy of lithium or how intracellular synthesis of *myo*-inositol impacts the normal development of the brain and other organs. To clarify

* This work was supported by in part by grant-in-aid from the Ministry of Education, Culture, Sports, Science and Technology of Japan (to T. O. and T. Y.), RIKEN BSI funds, grants from the Mitsubishi Pharma Research Foundation (to T. Y.), Astra Zeneca (to T. O.), Takeda Science Foundation (to T. O.), JSPS KAKENHI Grants 15200032 (to Y. G.), 21240043 (to Y. G. and T. M.), and 25241016 (to Y. G.), and grant-in-aid for scientific research on innovative areas (Unraveling the Micro-endophenotypes of Psychiatric Disorders at the Molecular, Cellular and Circuit Levels) from the Ministry of Education, Culture, Sports, Science and Technology (to T. Y.). A portion of this study is the result of the "Development of Biomarker Candidates for Social Behavior" Project carried out under the Strategic Research Program for Brain Sciences from Ministry of Education, Culture, Sports, Science and Technology (to T. Y.).
[S] This article contains supplemental Movie 1.
[1] To whom correspondence should be addressed. Tel.: 81-48-467-5946; Fax: 81-48-467-5946; E-mail: tohnishi@brain.riken.jp.

[2] The abbreviations used are: IMPase, *myo*-inositol monophosphatase; ENU, *N*-ethyl-*N*-nitrosourea; RGDMS, RIKEN ENU-based gene-driven mutagenesis system; DD, constant darkness.

this point, establishing reliable animal models in which the biological effects of inositol depletion are easily detectable as phenotypes is essential.

The potent mutagen, *N*-ethyl-*N*-nitrosourea (ENU) primarily causes single base substitutions. We generated a library of ENU-mutated mice and employed a high throughput screening system to detect mutations. We refer to these techniques collectively as RIKEN ENU-based gene-driven mutagenesis system (RGDMS) (15–18). Using RGDMS to generate and analyze mice with ENU-induced mutations, we uncovered unexpected functions for *Impa1* in the development of the skull, as well as in mouse behavior.

EXPERIMENTAL PROCEDURES

Mice—All protocols using animals were approved by the Animal Experiment Committee of RIKEN. Mice were housed in groups under constant temperature and humidity with a 12-h light/dark cycle (lights on at 08:00 h). They had *ad libitum* access to standard lab chow and water. In the rescue experiment, 2% *myo*-inositol in drinking water was provided to dams until weaning.

Screening of the ENU Mutant Mouse Library—The basic concept of our mutant mouse screening system (RGDMS) is shown in Fig. 1*A*. The library for *Impa* mutant mice was screened by PCR using the primer sets, followed by temperature gradient capillary electrophoresis. The information for used primers is available upon request. The mutations identified by temperature gradient capillary electrophoresis were confirmed by Sanger sequencing. Ova from normal mice were fertilized *in vitro* with sperm stocks harboring one of the identified missense mutations, and the zygotes were implanted in the uteri of female mice to create heterozygous (G2) mice. Founder mice were crossed at least six times with inbred C57BL/6N females (Japan SLC, Shizuoka, Japan) to dilute the original genetic background and irrelevant mutations. Heterozygous males and females were mated to generate homozygotes. The mutant strains are available from the RIKEN BioResource Center under the RBRC numbers shown in Table 1.

Genotyping of Mutant Mice—Genotyping of the *Impa1* missense mutants (F81L, T95K, and T96A) was performed as follows: genomic DNA purified from mouse tails was amplified using the primer set forward primer 5′-CTTCATCGTGTTTATTATTATCATCCTC-3′ and reverse primer: 5′-TTGGTCCCTTGCTCCACAGCTTAGA-3′. Amplicons were sequenced directly, using the forward primer and the BigDye Terminator Version 3.1 cycle Sequencing kit (Invitrogen).

In Vitro Enzyme Assays of Recombinant Proteins—IMPase assays were performed as described (8). In brief, a DNA fragment spanning the open reading frame of mouse *Impa1* was amplified from mouse brain Marathon-Ready cDNA (TaKaRa Bio, Ohtsu, Japan), using the primer set mIM1-Fw1, 5′-GTGCGCTCGCGCGAGATAATGGCAGAC-3′, and mIM1-Rv1, CCCAGGGACAGCAAGGATGACACTGGA-3′, followed by a second PCR assay with the primer set mIM1cds-Fw-EcoRV, 5′-AGTGAGATATCAATGGCAGACCCTTGGCAGGAG-3′, and mIM1cds-Rv-XhoI, AGTGACTCGAGCTAGCTTTCGTCGTCTCTTTG-3′ (underline sequences denote restriction enzyme recognition sites) to introduce restriction enzyme recognition sites into the PCR product. After digestion with EcoRV and XhoI, the resultant fragment was cloned into the EcoRV/XhoI site of SR-HA, a mammalian expression vector (19) that expresses proteins with N-terminal HA tags, generating SR-HA-mImpa1 WT. Site-directed mutagenesis following the standard DpnI method was performed to produce the three *Impa1* mutant constructs as follows: SR-HA-mImpa1 F81L, SR-HA-mImpa1 T95K, and SR-HA-mImpa1 T96A. The nucleotide sequence of each construct was verified. Human kidney-derived HEK293T cells were transfected with one these three constructs or SR-HA (empty vector), using the calcium phosphate method, and then cultured for 2 days. The HA-tagged recombinant proteins were purified from lysates to near-homogeneity using HA antibody affinity beads. Protein preparations were analyzed using SDS-PAGE, followed by silver staining and Western blotting with an anti-HA antibody.

Bone and Neurofilament Staining—T95K heterozygous male and female mice were intercrossed, and pregnant females were euthanized by cervical dislocation at E10.5, E14.5, or E18.5. Fetuses were removed quickly from uteri, and the tissue samples were harvested. E18.5 and E14.5 fetuses were stained with Alcian blue and alizarin red (20) to visualize bones. E10.5 embryos were subjected to whole-mount immunohistochemistry using an anti-neurofilament antibody (clone 2H3, Developmental Studies Hybridoma Bank, Iowa City, IA) and standard procedures to visualize neural fiber organization. Immune complexes were detected using a combination of anti-mouse IgG labeled with horseradish peroxidase and 3,3′-diaminobenzidine. Western blotting of the tissue extract was performed as described (8). Hematoxylin and eosin staining of brain paraffin sections was performed according to a standard procedure.

Behavioral Tests—Mice were 3–5 months old when tested. Behavioral tests were conducted as described (21, 22), except for circadian rhythm, which was evaluated using a wheel-running apparatus (23) with minor modifications. In brief, individual mice were housed in cages (28 cm wide × 12 cm deep × 15 cm high) equipped with a steel wheel (5.5 cm wide × 15 cm in diameter). For the assessment of circadian rhythm, wheel-running activity was monitored using a computer (O'Hara & Co., Tokyo, Japan) during regular light-dark cycles. Light intensity was set to 150 lux. The ClockLab software (Actimetrics, Wilmette, IL) was used to determine the circadian period.

Statistical Analysis—We used Student's *t* test to compare the two groups subjected to behavioral examinations. When data show a biased distribution, the nonparametric (Mann-Whitney *U*) test was used. When necessary, data were analyzed using two-way repeated measures analysis of variance followed by post hoc Fisher's protected least significant difference test. The segregation ratio of pup genotypes was tested for significance using the χ^2 test. A p value <0.05 was defined as significant.

RESULTS

Screening of the ENU mouse library for mutations in coding exons and flanking intron sequences of *Impa1* and *Impa2* (Fig. 1*A*) led to the identification of 17 mutations (12 in *Impa1* and 5 in *Impa2*) (Table 1), of which four were missense (nonsynonymous) mutations (*Impa1*: F81L, T95K, and T96A; *Impa2*: I282T) (Fig. 1, *B* and *C*, and Table 1). The Ile-282 residue is conserved between human and mouse IMPase homologs (Fig.

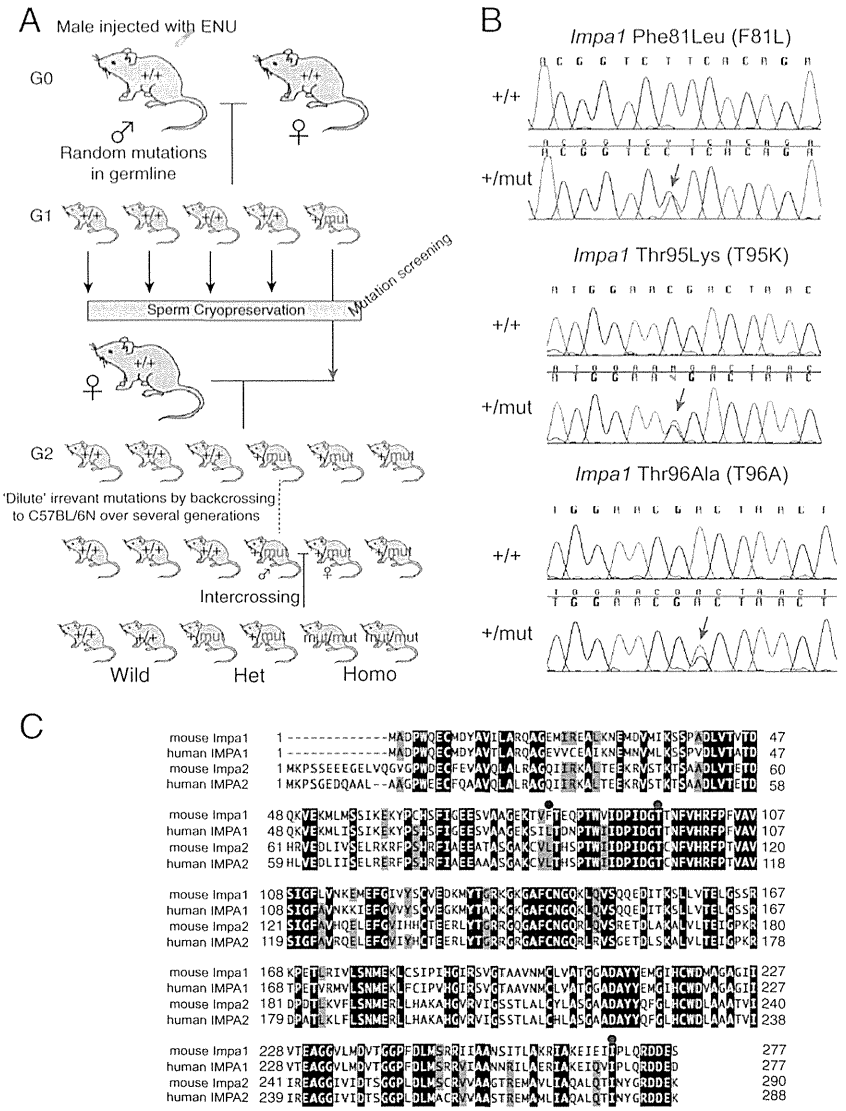

FIGURE 1. **ENU-induced mutations in *Impa1*.** *A*, schematic representation of the gene-driven ENU mutagenesis system. The library was screened for mutations in the two IMPase genes. *B*, sequence data for genomic DNA from three *Impa1* mutants. Note that each mutant strain (*G0*) is a heterozygote for the corresponding mutation. *Arrows* indicate the position of the mutation. *C*, amino acid sequence alignment of mouse and human IMPases. Identical and conserved amino acids are highlighted in *black* and *gray*, respectively. Positions of missense mutations are indicated by colored dots as follows: *blue*, *Impa1* Phe-81; *red*, *Impa1* Thr-95; *yellow*, *Impa1* Thr-96; and *green*, *Impa2* Ile-282.

1*C*, *green dot*), raising the possibility that it impacts the biological function of IMPase 2. However, because *Impa2* knock-out (KO) mice lack a detectable phenotype (21), we focused on the three *Impa1* mutations. In Fig. 2*A*, the positions of the mutant amino acid residues are mapped on the crystal structure of the mouse IMPase 1 homodimer (Protein Data Bank 4AS5) (24). The Thr-95 and Thr-96 residues (Fig. 1*C*, *red* and *yellow dots*, respectively) are close to the catalytic site, with Thr-95 being conserved between human and mouse IMPase homologs. The T95K mutation introduces a positive charge, potentially affecting conformation and enzymatic activity. In contrast, the substitution of Leu for Phe-81 may not have a deleterious effect as it is distant from the catalytic site and close to the surface (Fig. 2*A*). Moreover, Leu occupies a position corresponding to the mouse Impa1 Phe-81 residue in human IMPase 1 and IMPase 2 and in mouse IMPase 2 (Fig. 1*C*, *blue dot*). The PolyPhen-2 software tool (25) employs a three-step grading system to predict the impact of given mutations on the biological function of a protein as follows: benign, possibly damaging, and probably damaging. PolyPhen-2 predicted that the three missense mutations, F81L, T95K, and T96A, were benign, probably damaging, and possibly damaging, respectively (Table 1). These analyses strongly support the conclusion that the Lys-95 mutation may exert the strongest effect on biological function.

To test this possibility, wild-type and mutant HA-tagged IMPase 1 recombinant proteins were affinity-purified from cDNA-transfected HEK293T cells (Fig. 2*B*) and then tested for activity using a published method (8). Consistent with *in silico*

TABLE 1
Mutations identified in *Impa1* and *Impa2* genes

Gene	Mutant allele	Stock no.[a]	Position	Exon/intron	Amino acid change	PolyPhen-2
Impa1	Rgsc01422	RBRC-GD000153	c.85G>A	Intron 1		
	Rgsc01496	RBRC-GD000155	c.44T>A	Intron 1		
	Rgsc01494	RBRC-GD000154	c.63 + 46G>A	Intron 2		
	Rgsc01411[b]	RBRC-GD000162	c.197 + 55C>T	Intron 3		
	Rgsc00210	RBRC-GD000158	c.241T>C	Exon 4	F81L	Benign
	Rgsc01846	RBRC-GD000159	c.284C>A	Exon 4	T95K	Probably damaging
	Rgsc01827	RBRC-GD000160	c.286A>G	Exon 4	T96A	Possibly damaging
	Rgsc01639	RBRC-GD000157	c.322T>C	Exon 4	Synonymous	
	Rgsc01835	RBRC-GD000161	c.302 + 94G>A	Intron 4		
	Rgsc01418	RBRC-GD000151	c.303–4T>A	Intron 4		
	Rgsc01495	RBRC-GD000156	c.458–101A>G	Intron 6		
	Rgsc01423	RBRC-GD000152	c.566 + 43C>T	Intron 7		
Impa2	Rgsc01365	RBRC-GD000146	c.103–62C>T	Intron 1		
	Rgsc01384	RBRC-GD000149	c.342–29A>G	Intron 3		
	Rgsc01373	RBRC-GD000150	c.387 + 21T>C	Intron 4		
	Rgsc01363	RBRC-GD000147	c.496 + 85C>T	Intron 5		
	Rgsc01362	RBRC-GD000148	c.845T>C	Exon 8	I282T	Possibly damaging

[a] Mutant strains are available from RIKEN BioResource Center.
[b] This mutation was found in other G1 mice derived from the same G0 male, indicating that this mutation existed in the G0 male and was transmitted to G1 mice.

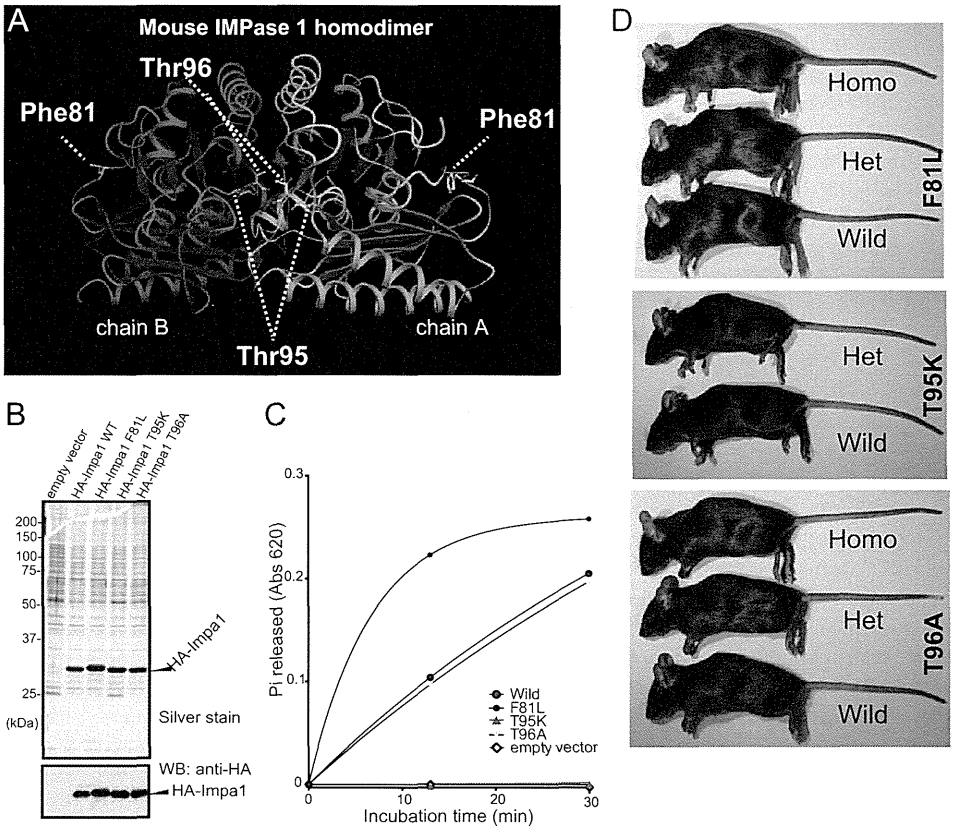

FIGURE 2. **T95K mutation inactivates the intrinsic activity of IMPase 1.** *A*, three-dimensional structure of the mouse IMPase 1 homodimer (Protein Data Bank code 4AS5) (*chains A* and *B*), showing the mutant amino acid residues. The CueMol software was used for the three-dimensional model construction. The Thr-95 and Thr-96 residues are located proximal to the enzyme catalytic site. *B*, recombinant HA-tagged IMPase 1 proteins purified from cDNA-transfected HEK293 cells were analyzed using SDS-PAGE, followed by silver staining. Western blot (*WB*) data using an anti-HA antibody is shown in the *lower panel*. Each sample contained equal loadings of recombinant protein. *C*, kinetics of phosphatase activity. Enzymatic activity of the T95K mutant (*red line*) was undetectable. *D*, lateral views of wild-type control (*Wild*), heterozygote (*Het*), and homozygote (*Homo*) mice. Homozygous T95K mice rarely survived into adulthood.

results, the Lys-95 (T95K) mutant lacked detectable activity (Fig. 2*C*). In contrast, there was no significant difference between the activity of wild-type and Ala-96 (T96A) proteins. Interestingly, the Leu-81 (F81L) mutant produced higher activity compared with the wild-type protein.

Next, we investigated the phenotypes of mice harboring these three mutations. Heterozygous mice (G (generation) 2 mice shown in Fig. 1*A*) were generated by *in vitro* fertilization. We detected no abnormalities in the heterozygotes (data not shown). Therefore, they were backcrossed to the inbred